

NONLINEAR CONTROL DESIGN FOR OPTIMAL DRUG DELIVERY IN MIXED CHEMO-IMMUNOTHERAPY: A ROBUST APPROACH FOR CANCER TREATMENT



By

Sheikh Asfand Yar Ali

(Registration No. 00000359914)

School of Interdisciplinary Engineering & Sciences
National University of Sciences and Technology (NUST)

Islamabad, Pakistan

February 2025

NONLINEAR CONTROL DESIGN FOR OPTIMAL DRUG DELIVERY IN MIXED CHEMO-IMMUNOTHERAPY: A ROBUST APPROACH FOR CANCER TREATMENT



By

Sheikh Asfand Yar Ali

(Registration No. 00000359914)

Supervisor

Dr. Absaar Ul Jabbar

A thesis submitted to the National University of Sciences and
Technology, Islamabad, in partial fulfillment of the
requirements for the degree of Master of Science
in Computational Science and Engineering

School of Interdisciplinary Engineering & Sciences


National University of Sciences and Technology (NUST)


Islamabad, Pakistan

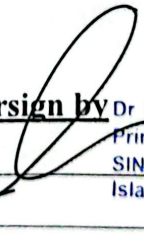
February 2025

THESIS ACCEPTANCE CERTIFICATE

Certified that final copy of MS/MPhil thesis written by Mr/Ms **SHEIKH ASFAND YARALI** Registration No. **00000359914** of **SINES** has been vetted by undersigned, found complete in all aspects as per NUST Statutes/Regulations, is free of plagiarism, errors, and mistakes and is accepted as partial fulfillment for award of MS/MPhil degree. It is further certified that necessary amendments as pointed out by GEC members of the scholar have also been incorporated in the said thesis.

Signature with stamp:  **Assistant Professor
SINES - NUST, Sector H-12
Islamabad**
Name of Supervisor: Dr. Abrar Ul Jabbar
Date: 13-02-2025

Signature of HoD with stamp:  **Dr. Mian Ilyas Ahmad
HoD Engineering
Professor
SINES - NUST, Sector H-12
Islamabad**
Date: 13/02/2025

Countersign by  **Dr. SYED IRTIZA ALI SHAH
Principal & Dean
SINES - NUST, Sector H-12
Islamabad.**
Signature (Dean/Principal): _____
Date: 13/2/25

Dedication

I dedicate this thesis to my father, who always encouraged me to move forward but is no longer in this world, and to my mother, whose words and prayers give me strength. To my siblings, who are always there for me in difficult times.

Declaration of Originality

I, Sheikh Asfand Yar Ali, solemnly declare that my MS thesis entitled **NONLINEAR CONTROL DESIGN FOR OPTIMAL DRUG DELIVERY IN MIXED CHEMO-IMMUNOTHERAPY: A ROBUST APPROACH FOR CANCER TREATMENT** represents my independent work. This thesis has not been submitted previously for the fulfillment of any degree at the National University of Sciences and Technology (NUST), Pakistan, or any other academic institution globally.

I affirm the originality of my work, and at any time if my statement is found to be incorrect even after my post-graduation, the university has the right to withdraw my MS degree.

Sheikh Asfand Yar Ali
00000359914

Copyright Notice

- Copyright in text of this thesis rests with the student author. Copies (by any process) either in full, or of extracts, may be made only in accordance with instructions given by the author and lodged in the Library of SINES, NUST. Details may be obtained by the Librarian. This page must form part of any such copies made. Further copies (by any process) may not be made without the permission (in writing) of the author.
- The ownership of any intellectual property rights which may be described in this thesis is vested in SINES, NUST, subject to any prior agreement to the contrary, and may not be made available for use by third parties without the written permission of SINES, which will prescribe the terms and conditions of any such agreement.
- Further information on the conditions under which disclosures and exploitation may take place is available from the Library of SINES, NUST, Islamabad.

Acknowledgments

Alhamdulillah!

I am truly grateful to Allah for providing me with the strength, resilience, and opportunities to reach this academic milestone. His guidance has always motivated me. I want to express my gratitude to my family for their support throughout this journey. Their belief in me has been essential for achieving my goals.

I extend my sincere appreciation to my supervisor, Dr. Absaar Ul Jabbar, from the School of Interdisciplinary Engineering and Sciences at NUST. His consistent assistance, insightful advice, and constructive feedback have been essential throughout my studies.

I recognize the School of Interdisciplinary Engineering and Sciences faculty members for their wisdom and encouragement, which have greatly helped my academic growth. Their passion for teaching and research has created a great learning environment.

Contents

1	Introduction	1
1.1	Cancer and Its Stages	1
1.1.1	Types of Cancer	1
1.1.2	Stages of Cancer	2
1.1.3	Cancer Statistics	2
1.2	Treatment Methods and Side Effects	4
1.2.1	Mixed Chemo-Immunotherapy	5
1.2.2	Side Effects of Mixed Chemo-Immunotherapy	5
1.3	Control Strategies in Cancer Treatment	6
1.4	Problem Statement	6
1.5	Contribution	6
1.6	Research Objectives:	7
1.7	Outline	7
2	Literature Review	8
2.1	Mathematical Models in Cancer Treatment	8
2.1.1	Chemotherapy	8
2.1.2	Immunotherapy	9
2.1.3	Mixed Chemo-Immunotherapy	11
2.1.4	Nonlinear Tumor Model	11
3	Controller Utilization And Methodology	16
3.1	Robust Controller Design	16
3.1.1	Terminal Sliding Mode Controller Design	16
3.1.2	Super Twisting Sliding Mode Controller Design	23
3.2	Adaptive Controller Design	27
3.2.1	Adaptive Terminal Sliding Mode Controller Design	27
3.2.2	Adaptive Super Twisting Sliding Mode Controller Design	35
3.3	Controller Optimization	41
4	Results And Discussion	45
4.1	Comparison of Robust Controllers	46
4.1.1	Tumor Cell Comparison	46
4.1.2	Natural Killer Cell Comparison	46
4.1.3	CD8 ⁺ T Cell Comparison	47
4.1.4	Circulating Lymphocytes Comparison	48
4.1.5	Chemotherapy Concentration Comparison	49
4.1.6	Immunotherapy Concentration Comparison	49
4.1.7	Drug Delivery Scenario	50

4.2	Hardware-in-loop	52
4.2.1	Hardware-in-Loop Simulation Results	53
4.2.2	Benefits of Hardware-in-the-Loop (HIL)	58
5	Conclusion And Future Directions	59
5.1	Conclusion	59
5.2	Scopes and Limitations	59
5.3	Further Research Work	60
	Bibliography	61

List of Tables

2.1	HUMAN PARAMETER VALUES (PATIENT 9)	15
3.1	Optimized Gains and Costs for TSMC and ATSMC	44
3.2	Optimized Gains and Costs for STSMC and ASTSMC	44
4.1	Initial Conditions of States	45
4.2	Limits (Bounds) of Control Variables	45
4.3	Convergence of States (in Days) Under Different Controllers	52

List of Figures

1.1	New cases of Cancer in 2022 (For all ages and genders)	3
1.2	Cancer Deaths in 2022 (For all ages and genders)	4
2.1	The schematic diagram depicts the interactions and effects of natural killer cells, $CD8^+$ T cells, circulating lymphocytes, chemotherapy, and immunotherapy on tumor cells.	14
3.1	Decreasing Trend of MSE Cost Function for Different Controllers	43
4.1	Tumor Cell Population Comparison Over Time.	46
4.2	Natural Killer Cell Population Comparison Over Time.	47
4.3	$CD8^+$ T Cell Population Comparison Over Time.	48
4.4	Circulating Lymphocytes Population Comparison Over Time.	48
4.5	Chemotherapy Concentration Comparison Over Time.	49
4.6	Immunotherapy Concentration Comparison Over Time.	50
4.7	Comparison of Drug Delivery Scenarios Across Controllers.	51
4.8	HIL Simulation System Display	53
4.9	Tumor Cell Population Comparison Over Time.	54
4.10	Natural Killer Cell Population Comparison Over Time.	54
4.11	$CD8^+$ T Cell Population Comparison Over Time.	55
4.12	Circulating Lymphocytes Population Comparison Over Time.	55
4.13	Chemotherapy Concentration Comparison Over Time.	56
4.14	Immunotherapy Concentration Comparison Over Time.	56
4.15	Immunotherapy Dosage (TIL): $v_L(t)$ Comparison Over Time.	57
4.16	Chemotherapy Dosage: $v_M(t)$ Comparison Over Time.	57
4.17	Immunotherapy Dosage (IL-2): $v_I(t)$ Comparison Over Time.	58

Abstract

Mixed chemo-immunotherapy is an effective strategy for cancer treatment. This study utilizes a six-state nonlinear mathematical model to describe the dynamics of tumor growth and immune responses during mixed chemo-immunotherapy. The model incorporates key components, including tumor cells (T), natural killer cells (N), CD8⁺T cells (L), circulating lymphocytes (C), chemotherapy concentration (M), and immunotherapy concentration (I). Advanced nonlinear controllers such as Terminal Sliding Mode Control (TSMC), Super Twisting Sliding Mode Control (STSMC), Adaptive Terminal Sliding Mode Control (ATSMC), and Adaptive Super Twisting Sliding Mode Control (ASTSMC) are proposed to optimize drug delivery and achieve rapid tumor regression. These controllers ensure drug dosages remain within safe toxicity limits while minimizing side effects and supporting immune system recovery. To fine-tune the gain parameters of these controllers, the Improved Grey Wolf Optimization (IGWO) algorithm is employed with the Mean Squared Error (MSE) as the cost function. The stability of these controllers is rigorously analyzed using Lyapunov-based stability theory, ensuring reliable performance during treatment. The proposed controllers are simulated in MATLAB/Simulink and further validated through a hardware-in-the-loop (HIL) experimental setup using the C2000 Delfino™ MCU F28379D Launchpad, confirming the practicality and effectiveness of the proposed approach. Simulation results show that ASTSMC achieves tumor regression in just 9 days, approximately 5.42 times faster than the previous study (48.77 days), while maintaining safe toxicity limits and ensuring optimal drug dosages.

Keywords: Chemotherapy, Immunotherapy, Biomedical Control, Mixed cancer therapy Sliding mode control, Tumor

Chapter 1

Introduction

1.1 Cancer and Its Stages

Cancer is a group of diseases where cells in the body begin to grow and divide in an irregular way. This growth can occur in different organs and tissues, often leading to significant health challenges. Early detection and effective treatment are key factors in improving survival and quality of life for patients. Despite advancements in research and treatment, cancer continues to be one of the leading causes of death worldwide.

1.1.1 Types of Cancer

There are various types of cancer, each affecting different parts of the body and requiring unique approaches for diagnosis and treatment:

- **Sarcomas:** Rare cancers arising in connective tissues like bones, muscles, and fat. They are aggressive and require early detection for better outcomes.
- **Leukemia:** A cancer of the bone marrow, leading to overproduction of abnormal white blood cells that impair the body's ability to fight infections.
- **Lymphomas:** Cancers of the lymphatic system, including Hodgkin and non-Hodgkin lymphoma, affecting lymph nodes and the immune system.
- **Melanomas:** A type of skin cancer that arises from pigment-producing cells and can spread quickly if not treated early.
- **Brain and Spinal Cord Cancers:** Cancers that develop in the brain or spinal cord, often leading to neurological symptoms and requiring complex treatment.
- **Gastrointestinal Cancers:** Cancers affecting the digestive system, including the colon, stomach, and pancreas, often diagnosed late due to subtle symptoms.
- **Endocrine Cancers:** Cancers that affect hormone-producing glands like the thyroid and pancreas, disrupting hormonal balance and causing various symptoms.
- **Urological Cancers:** Cancers affecting the urinary system, including the kidneys, bladder, and prostate, often detected through urinary symptoms or imaging.
- **Respiratory Cancers:** Cancers of the lungs and respiratory system, with lung cancer being the most common and deadly, often linked to smoking.

1.1.2 Stages of Cancer

The staging of cancer plays a vital role in assessing the extent of the disease and is crucial for planning effective treatment and predicting outcomes. Stages range from localized conditions to advanced cases where the cancer has spread to other parts of the body. The following are the stages of cancer:

- **Stage 0:** Also known as carcinoma in situ, this is an early stage where cancer cells are present but have not spread beyond the original tissue. The tumor is localized and often curable with minimal intervention.
- **Stage I:** The cancer is still localized within its original tissue and has not spread to nearby lymph nodes or distant areas. This stage is typically considered an early, more treatable stage of cancer.
- **Stage II:** The cancer has grown larger or spread to nearby tissues, but it remains confined to the primary site. It may involve nearby lymph nodes or organs, depending on the type of cancer. Treatment may involve surgery or radiation.
- **Stage III:** The cancer has spread more extensively within the local area, often involving nearby lymph nodes or distant tissues but not yet reaching distant organs. At this stage, the cancer is more aggressive, and treatment may include a combination of surgery, chemotherapy, radiation, or targeted therapies.
- **Stage IV:** Known as metastatic cancer, it has spread to distant parts of the body, such as the bones, lungs, liver, or brain. This stage is often more difficult to treat and focuses on managing symptoms and prolonging life through advanced treatments like chemotherapy, immunotherapy, or palliative care.
- **Recurrent:** Cancer that has returned after treatment, either at the original site or in a new location. Treatment options depend on the location of the recurrence and may include surgery, chemotherapy, or radiation to manage the disease.

1.1.3 Cancer Statistics

Cancer is a prevalent and significant health concern that impacts the lives of millions of individuals across the globe, posing substantial challenges for patients, families, and health-care systems [6]. As highlighted in the cancer report by the World Health Organization (WHO) [16], [17], cancer is recognized as the second leading cause of death globally, underscoring its profound effect on public health. In 2022, an estimated 19.3 million new cases of cancer were recorded worldwide. Among these cases, lung cancer comprised 12.4%, breast cancer 11.5%, colorectal cancer 9.6%, and prostate cancer 7.3%. Stomach and liver cancers accounted for 4.8% and 4.3%, respectively, while all other types made up 49.9% (see Figure 1.1).

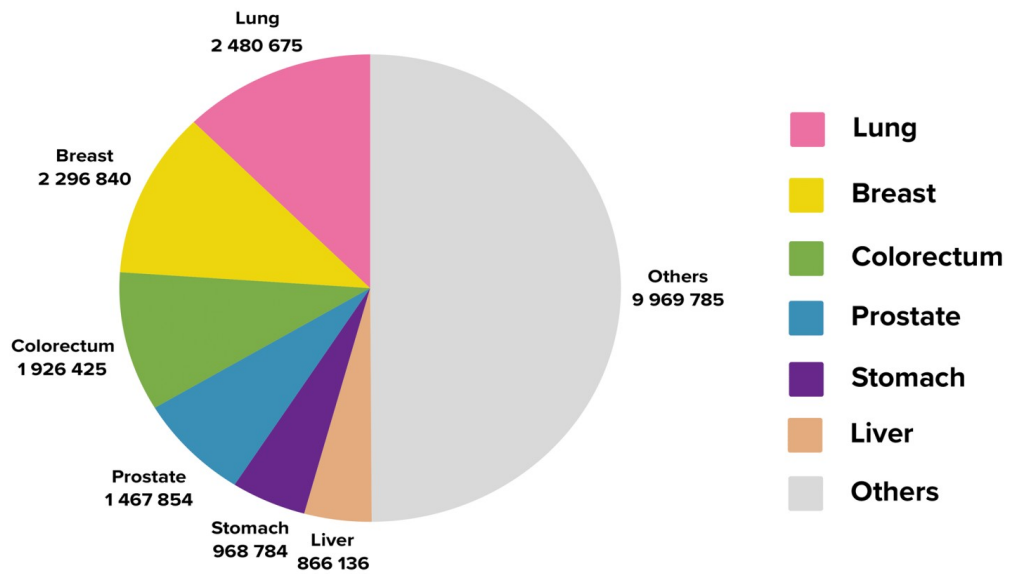


Figure 1.1: New cases of Cancer in 2022 (For all ages and genders)

With 10 million cancer-related deaths in 2022 (see Figure 1.2), the disease continues to cause considerable global mortality. Lung cancer accounted for 18.7% of these deaths, while colorectal cancer made up 9.3%, liver cancer 7.8%, breast cancer 6.8%, stomach cancer 6.8%, and pancreatic cancer 4.8%. Other types of cancer contributed to 45.9% of the total deaths. The situation is similarly alarming in Pakistan, where approximately 207,000 new cancer cases were reported in the same year, resulting in nearly 160,000 cancer-related fatalities [2]. These numbers emphasize the urgent need for improved prevention, early detection, and treatment, both globally and in countries like Pakistan.

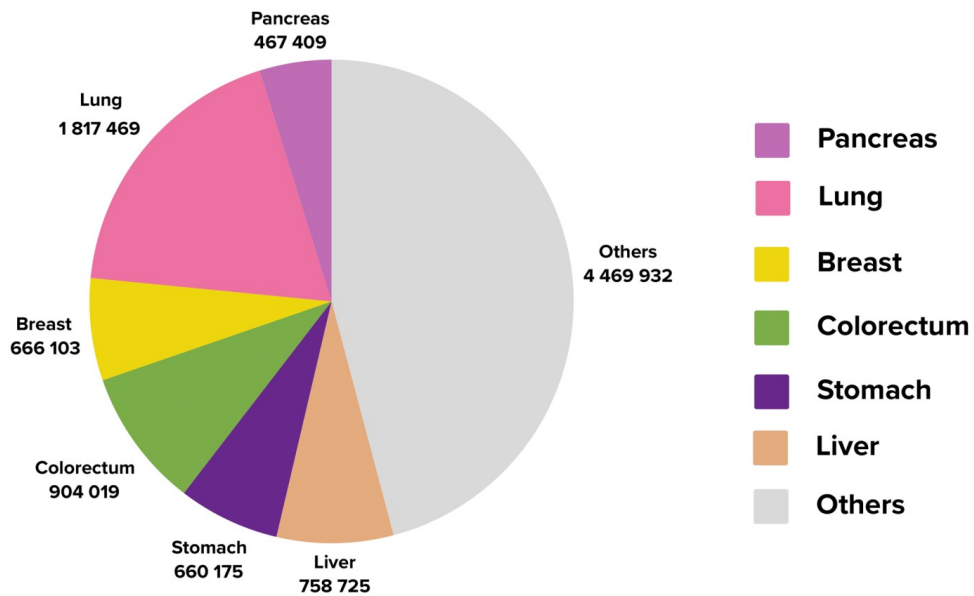


Figure 1.2: Cancer Deaths in 2022 (For all ages and genders)

1.2 Treatment Methods and Side Effects

The treatment of cancer involves various methods, including radiotherapy, immunotherapy, surgery, and chemotherapy, often combined to increase their effectiveness depending on the type and stage of the disease.

- Chemotherapy, as a mainstay of cancer treatment, employs powerful cytotoxic drugs to target rapidly dividing cancer cells throughout the body. While effective at destroying cancer cells, these drugs can also affect healthy cells that divide quickly, such as those in hair follicles, bone marrow, and the digestive tract. This non-selective action leads to well-known side effects including hair loss, decreased blood cell counts, nausea, and fatigue. Modern chemotherapy protocols have been refined to maximize effectiveness while minimizing adverse effects through careful dosing schedules and supportive care measures.
- Immunotherapy has emerged as a revolutionary approach that harnesses the body's immune system to fight cancer. This treatment works by either stimulating the immune system's natural ability to attack cancer cells or providing synthetic immune system components to enhance the anti-cancer response. Various types of immunotherapy include checkpoint inhibitors, CAR T-cell therapy, and cancer vaccines, each working through different mechanisms to strengthen the body's natural defenses against cancer.
- Radiation therapy utilizes high-energy radiation beams like super-powerful X-rays, to destroy the DNA of cancer cells, preventing them from growing and dividing. This treatment can be delivered externally (external beam radiation) or internally (brachytherapy). The process usually involves multiple sessions over days or weeks

to achieve the desired results. Modern radiation techniques like intensity-modulated radiation therapy (IMRT) and stereotactic body radiation therapy (SBRT) allow for highly precise delivery of radiation, minimizing damage to healthy tissues while maximizing the dose to the tumor.

- Hormone therapy is particularly important in treating hormone-sensitive cancers such as breast and prostate cancer. This treatment works by either blocking the body's ability to produce specific hormones or interfering with how hormones behave in the body, thereby slowing or stopping the growth of hormone-dependent cancer cells. For breast cancer, the treatment works by either blocking estrogen receptors using drugs like tamoxifen (SERMs) or preventing estrogen production through aromatase inhibitors. In prostate cancer, the therapy focuses on reducing testosterone levels through medications or surgery.
- Surgery therapy is a fundamental approach in cancer treatment where skilled surgeons physically remove cancerous tissues from the body. The primary goal is to eliminate the tumor and some surrounding healthy tissue (called margins) to ensure all cancer cells are removed.

1.2.1 Mixed Chemo-Immunotherapy

One of the promising methods is mixed chemo-immunotherapy, which combines chemotherapy and immunotherapy. In this treatment, chemotherapy directly attacks and kills cancer cells, while immunotherapy helps strengthen the body's natural defenses to fight cancer. Together, they work in tandem, making the treatment more powerful than when used separately.

This combined method has shown positive results in many studies [19, 5, 15, 23]. While chemotherapy can sometimes weaken the immune system, adding immunotherapy helps keep the immune response strong, improving the body's ability to fight cancer. Many patients have had better outcomes with this combined treatment than with chemotherapy alone.

1.2.2 Side Effects of Mixed Chemo-Immunotherapy

While combining chemotherapy and immunotherapy has shown potential in improving cancer treatment outcomes, there are some important drawbacks to consider. One major concern is the increased risk of severe immune-related side effects (irAEs). These side effects occur when the immune system, stimulated by immunotherapy, mistakenly targets healthy tissues. Symptoms of irAEs can include inflammation, rashes, fatigue, and fever, which may cause discomfort for patients. In more severe cases, these side effects can become life-threatening, requiring immediate medical intervention.

Another challenge is that chemotherapy can weaken the immune system, making patients more susceptible to these immune-related side effects. While chemotherapy targets cancer cells, it also reduces the body's ability to fight off infections and inflammation, complicating the response to immunotherapy and increasing the risk of irAEs.

Thus, although the combination of chemotherapy and immunotherapy can improve cancer treatment, it also requires careful monitoring to manage the potential risks.

1.3 Control Strategies in Cancer Treatment

Control strategies have emerged as crucial tools in modern cancer treatment, allowing for the optimization of therapeutic regimens while managing the complexities associated with cancer therapy. The dynamic nature of cancer, marked by tumor growth, immune system responses, and drug interactions, makes it difficult to deliver successful treatments. Control theory, particularly nonlinear control methods, offers a robust framework for managing these complexities and improving patient outcomes.

One of the primary applications of control strategies in cancer treatment is the optimization of drug delivery. Drugs must be carefully administered to ensure they reach therapeutic levels that effectively target tumor cells while minimizing toxicity. Control strategies enable the adjustment of drug dosages in real-time, taking into account the tumor's growth, immune system activity, and the pharmacokinetics of the drugs involved. This dynamic adjustment facilitates the delivery of drugs at optimal concentrations, maximizing their tumor-killing effects while minimizing harmful side effects.

The control systems are categorized into linear and nonlinear types. Linear control assumes proportional relationships between inputs (e.g., drug dosage) and outputs (e.g., therapeutic effects) while nonlinear control techniques are well-suited for cancer treatment because of the unpredictable and nonlinear characteristics of biological systems. Methods such as sliding mode control (SMC) and various adaptive methods have been successfully implemented to manage drug delivery systems. These techniques enable quick adjustments and provide stability against uncertainties in the system, such as changes in tumor behavior or patient-specific factors. By incorporating these advanced control methods, cancer treatments can be more accurately tailored to individual patients, leading to better therapeutic results.

1.4 Problem Statement

The challenge of minimizing drug dosage and treatment time in mixed chemo-immunotherapy remains a critical concern, as excessive dosages can lead to toxicity and severe side effects. This study utilizes advanced nonlinear controllers such as Terminal Sliding Mode Control (TSMC), Super Twisting Sliding Mode Control (STSMC), Adaptive Terminal Sliding Mode Control (ATSMC), and Adaptive Super Twisting Sliding Mode Control (ASTSMC) to optimize drug delivery and achieve rapid tumor regression while maintaining safe toxicity limits. The gain parameters of these controllers are optimized using the Improved Grey Wolf Optimization (IGWO) algorithm to enhance performance. The proposed approach is validated through Lyapunov-based stability analysis and MATLAB/Simulink simulations, ensuring its effectiveness in improving cancer treatment.

1.5 Contribution

The robust nonlinear controllers, which are adaptive variants of Sliding Mode Control (SMC), are utilized for efficient drug delivery in Mixed Chemo-Immunotherapy. To the best of my knowledge, these adaptive controllers have not been applied to this particular problem in the existing literature.

1.6 Research Objectives:

1. Study and analyze models from the literature
2. Implement control techniques and reproduce simulation results using MATLAB/Simulink
3. Evaluate system stability using Lyapunov Stability Theory
4. Apply Improved Grey Wolf Optimization (IGWO) to optimize control parameters
5. Perform Hardware-in-the-Loop (HIL) simulation for real-time validation
6. Compare the results with each other

1.7 Outline

The forthcoming chapters outline the study's framework, methods, findings, and future directions in a sequential arrangement. Chapter 2 presents a literature review on the development and application of mathematical models in cancer treatment, focusing on chemotherapy, immunotherapy, and their combined strategies. Chapter 3 details the implementation of advanced control strategies, including TSMC, STSMC, ATSMC, and ASTSMC, to control tumor growth while minimizing drug usage and treatment duration in chemo-immunotherapy. Chapter 4 discusses simulations and results. Chapter 5 delves into future directions and provides the conclusion.

Chapter 2

Literature Review

This chapter outlines the development of cancer treatments, focusing on the combination of chemotherapy and immunotherapy. Initially introduced in earlier decades, these treatments have progressed over time, reflecting advancements in their application. A review of key studies offers an overview of their use and identifies areas that require further investigation. This chapter also establishes a foundation for the subsequent chapters, providing a basis for the experiments and findings that examine the role of combined chemotherapy and immunotherapy in cancer care.

2.1 Mathematical Models in Cancer Treatment

Mathematical modeling plays a vital role in the analysis of cancer and its treatment. By creating mathematical representations of tumor growth and progression, researchers can simulate various biological processes that occur within the body. These models often use differential equations to describe how tumors evolve over time in response to internal and external factors. Through simulations, researchers can predict tumor behavior under different conditions, which aids in evaluating potential treatment strategies. The development of these models allows for the identification of key parameters that influence tumor behavior, enabling researchers to assess how changes in treatment protocols may affect outcomes. Additionally, mathematical models can incorporate real-time patient data, allowing for adjustments based on individual responses and addressing the variability seen in cancer cases. This capability supports the optimization of drug delivery systems by facilitating the examination of different dosing schedules and combinations of therapies. Furthermore, mathematical modeling contributes to a deeper understanding of cancer biology by clarifying the mechanisms underlying tumor growth and response to treatment. Overall, mathematical modeling serves as an essential tool for advancing research in cancer treatment and refining therapeutic methodologies.

2.1.1 Chemotherapy

Chemotherapy represents a class of cancer treatments that use drugs designed to stop or slow cancer cell growth. The treatment introduces chemical agents into the bloodstream to attack cells that divide rapidly - a key characteristic of cancer. However, this mechanism also affects normal fast-dividing cells throughout the body, leading to unintended effects on healthy tissues. Doctors must carefully plan drug amounts and timing to strike a balance between fighting cancer and protecting the patient's overall health. Mathematical models of chemotherapy have evolved substantially since the 1970s, progressing from basic tumor

growth equations to sophisticated control systems.

In 1973, Swan and Vincent [1] created one of the first mathematical frameworks incorporating Gompertzian growth equations and Monte Carlo simulations to study tumor kinetics during chemotherapy. This early work modeled cell cycle behavior and drug effects, though it assumed uniform tumor populations and simplified drug interactions. By 1994, advances in mathematical modeling [13] addressed optimal drug scheduling through direct search optimization techniques. The models solved constrained optimal control problems using differential equations to represent tumor growth and drug dynamics. This method reduced tumor size to 25,700 cells while maintaining drug concentrations within safe limits, achieving a 47% improvement over previous studies. The resulting drug schedule showed two peak periods of maximum drug concentration, demonstrating how mathematical optimization could guide treatment timing. We introduce adaptive and higher-order sliding mode controllers for dynamic, real-time control of drug delivery.

Recent studies [22] have introduced more complex modeling approaches with a four-state ordinary differential equation model capturing interactions between tumor cells, normal cells, immune cells, and chemotherapy drugs. This model incorporated logistic growth patterns and cell interaction parameters, allowing for more realistic representations of treatment dynamics. Our model includes additional variables, offering a more comprehensive representation of multidimensional treatment strategies.

Control theory applications in chemotherapy models have expanded to include various strategies. Research in [32] applied Sliding Mode Control (SMC) and its variants like Terminal Sliding Mode Control (TSMC) to brain tumor treatment models. These controllers aim to minimize tumor cells while preserving healthy tissue and reducing drug usage. Their research demonstrated that TSMC achieved rapid tumor reduction with minimal drug requirements, validated through Lyapunov stability analysis. Our work extends beyond TSMC by introducing ATSMC and ASTSMC for greater resilience and adaptive control.

Additional studies [31] examined Lyapunov redesign controllers and Terminal Sliding Mode Control, finding that TSMC eliminated control chattering while requiring less drug input compared to other methods. Further research [30] evaluated Backstepping and Synergetic controllers, with Backstepping achieving faster tumor reduction and maintaining zero steady-state error in the system response. We validate stability using Lyapunov theory and incorporate hardware-in-the-loop testing for real-time applicability, along with adaptive mechanisms to enhance control performance.

The progression of mathematical models in chemotherapy showcases increasing computational capabilities and biological understanding. Modern models consider multiple cell populations, drug pharmacokinetics, and system uncertainties, enabling more precise treatment planning and evaluation.

2.1.2 Immunotherapy

Immunotherapy works by activating and strengthening the body's natural defense mechanisms to identify and destroy cancer cells. Mathematical models help analyze the intricate interactions between immune system components and tumors, guiding treatment decisions and timing. In pioneering research [11], a system of ordinary differential equations (ODEs) modeled the dynamic relationships between tumor cells, immune effector cells, and interleukin-2 (IL-2). By incorporating Michaelis-Menten kinetics, the model represented saturation effects in immune responses and cytokine production. The research

showed how antigenicity - the tumor's ability to be recognized by the immune system - and immune response strength determined treatment outcomes. While this model added to understanding of tumor dormancy and recurrence through stable limit cycles, it did not account for spatial variations in tumor tissue or the roles of other immune components like regulatory T cells and macrophages. Vladimir [12] described cytotoxic T lymphocyte responses to immunogenic tumors through nonlinear ODEs. This research modeled the creation of effector cell-tumor cell conjugates and tracked how effector cells became inactive over time. The model matched experimental data from BCL1 lymphoma in chimeric mice, demonstrating cyclic patterns of tumor growth and reduction. The equations helped identify transitions between states of dormancy and uncontrolled tumor growth through bifurcation theory. However, the model relies on estimated parameters, assumes homogeneous effector populations, overlooks tumor heterogeneity, and lacks control strategies like nonlinear controllers.

Later, validated models [21] combined differential equations with experimental data to create a comprehensive picture of N and CD8⁺T cells behavior. The equations represented key biological processes: tumor cell growth, immune-driven destruction, and regulation through cytokine production. While mathematically rigorous, these models noted limitations in excluding factors like regulatory T cells and the tumor microenvironment. The complex equations, though accurate, posed challenges for real-time clinical applications.

Advanced modeling [20] built a three-equation system to represent interactions between tumor cells, natural killer (N) cells, and CD8⁺T cells. This model introduced new mathematical terms for immune-mediated killing, with N cells following traditional product forms while CD8⁺T cells used ratio-dependent functions that better matched experimental observations. The equations included baseline NK cell production, tumor-driven recruitment, and cell inactivation after prolonged tumor contact. The model also showed how ligand-transduced tumor cells could trigger stronger immune responses. The model overlooks spatial heterogeneities, relies on data-driven parameters with limited generalizability.

Further Babbs [3] created a mathematical framework based on predator-prey dynamics, where immune cells acted as predators and tumor cells as prey. Two differential equations formed the core of this model: one describing tumor cell growth affected by intrinsic growth and immune-mediated killing, and another representing immune cell dynamics influenced by tumor-immune interactions and immune cell decay. This work revealed oscillation patterns in cell populations and determined specific thresholds that separated successful treatments from failures. The model stressed the necessity of maintaining consistent immune stimulation over extended periods, as early stoppage of treatment could lead to poor outcomes. However, the simplification to a predator-prey system, while making the model more accessible, left out critical factors like tumor heterogeneity and immune resistance mechanisms.

Research focusing on dendritic cell vaccines [7] developed ODEs to track tumor-specific CD4 T helper cells, CD8 cytotoxic T cells, cancer cells with tumor-associated antigens, mature dendritic cells, and IL-2 cytokines. Through optimal control theory, the model calculated ideal injection schedules. The mathematics suggested an initial high-dose injection to rapidly decrease tumor size, followed by smaller periodic doses for maintenance. This hybrid control strategy balanced treatment effectiveness with patient safety considerations.

2.1.3 Mixed Chemo-Immunotherapy

Mixed chemo-immunotherapy combines chemotherapy and immunotherapy to fight cancer through complementary mechanisms, and we have applied this in our studies. Chemotherapy targets cancer cells by exploiting their high growth rate, while immunotherapy strengthens the body's natural defenses to identify and remove these cells. Mathematical models and clinical trials have focused on refining this combination to maximize its potential.

Mixed chemo-immunotherapy has drawn significant attention in therapeutic circles. For example, [28] unveiled synergistic patterns between chemotherapy and immunotherapy. While this work highlighted biological interplay, the absence of mathematical representations to quantify these interactions, reduced its utility for predicting outcomes or optimizing protocols.

Additional progress was made in feedback design and model updating, which expanded on De Pillis' model using nonlinear predictive control (NMPC) to dynamically modify therapy schedules [8]. While this effort handled certain uncertainties, it remained constrained by its reliance on simplified models and simulations. Adaptive inversion models used constrained optimization techniques to coordinate chemotherapy and immunotherapy, achieving tumor reduction and immune restoration [29]. However, the reliance on static parameter assumptions limited their relevance to real-world scenarios. Pulsed therapy models [24] considered periodic treatment regimens, showing that combined regimens outperformed monotherapies. Nevertheless, their limited flexibility in responding to real-time conditions and omission of cytokine interactions reduced their clinical applicability.

Multiple model predictive control [18] used an adaptive method to increase drug delivery to reduce tumor volume and support immune function. However, difficulties arose due to its emphasis on system homogeneity and precise parameter values, which limit its generalizability. Immunogenic chemotherapy [26] centered on medium-dose intermittent chemotherapy (MEDIC) to balance tumor suppression and immune activation, but did not account for mechanisms of real-time feedback or adaptability to individual patient needs. Developments in drug delivery systems [27] looked at technologies such as nanoparticles and hydrogels to optimize targeted delivery and reduce systemic toxicity. However, the absence of quantitative modeling hindered efforts to predict and adjust therapeutic results.

Lung cancer treatment combinations [10] pinpointed the interplay between conventional cytotoxic therapies and immune checkpoint blockers for non-small cell lung cancer. While this work decoded biological mechanisms, the lack of mathematical representations hampered broader implementation. A seven-state ODE architecture [9] yielded strategies to balance tumor reduction and immune system preservation. However, the rigid control design and fixed treatment schedules curtailed its adaptation to physiological fluctuations. A comprehensive nine-state immune-tumor model showed how immune regulators and cytokines work together, revealing complicated biological interactions. Yet, parameter estimation uncertainties and limited experimental validation created barriers to adoption. The merged immunotherapy-chemotherapy strategy [25] used Pontryagin's Maximum Principle to orchestrate treatment timing. Its homogeneous assumptions and computational nature, though, diminished its practical value in personalized medicine protocols.

2.1.4 Nonlinear Tumor Model

The six-state mathematical model established by de Pillis [19] served as the basis for many research efforts on mixed chemo-immunotherapy. The model encompassed tumor growth, immune responses involving natural killer cells, cytotoxic T lymphocytes, and circulating

lymphocytes, along with the effects of chemotherapy and immunotherapy agents. Ordinary differential equations were used to represent the nonlinear interactions between tumor cells and immune cells, as well as the changes brought about by treatment interventions. Our research built on this important model by using its parameters (see Table 2.1) and adding robust nonlinear controllers, such as Terminal Sliding Mode Control, Super Twisting Sliding Mode Control, Adaptive Terminal Sliding Mode Control, and Adaptive Super Twisting Sliding Mode Control, to achieve better treatment results.

State Variables:

The mathematical structure meticulously monitors:

- **Tumor Cell Population (T):** Depicts the cancer cell count, which multiplies through logistic growth and decreases through immune system attacks and therapeutic interventions.
- **Natural Killer Cells (N):** These innate immune system elements exist naturally in the body, sustaining their defensive role even without tumor detection. N cells serve as the first line of defense against cancer cells.
- **Cytotoxic T Lymphocytes (L):** Known as CD8⁺T cells, these specialized immune cells execute targeted responses against tumor cells. Their population shifts through various pathways such as tumor interaction, N cell modulation, and therapeutic activation.
- **Circulating Lymphocytes (C):** These embody the broader immune system elements, sustaining a baseline defense mechanism and bolstering the overall immune response.
- **Chemotherapy Concentration (M):** Measures the presence of cytotoxic agents in the system, which attack rapidly dividing cells such as tumor cells.
- **Immunotherapy Concentration (I):** Monitors IL-2 levels, this variable characterizes the immunotherapeutic agent that amplifies the body's natural immune response.

Mathematical Model:

The coupled differential equations describe the relationships between these state variables:

$$\frac{dT}{dt} = aT(1 - bT) - cNT - DT - k_T(1 - e^{-M})T, \quad (2.1)$$

$$\frac{dN}{dt} = eC - fN + g\frac{T^2}{h + T^2}N - pNT - k_N(1 - e^{-M})N, \quad (2.2)$$

$$\begin{aligned} \frac{dL}{dt} = & -mL + j\frac{D^2T^2}{k + D^2T^2}L - qLT + (r_1N + r_2C)T \\ & - uNL^2 - k_L(1 - e^{-M})L + \frac{pIL_I}{gI + I} + v_L(t), \end{aligned} \quad (2.3)$$

$$\frac{dC}{dt} = \alpha - \beta C - k_C(1 - e^{-M})C, \quad (2.4)$$

$$\frac{dM}{dt} = -\gamma M + v_M(t), \quad (2.5)$$

$$\frac{dI}{dt} = -\mu_I I + v_I(t), \quad (2.6)$$

$$D = d\frac{\left(\frac{L}{T}\right)^l}{s + \left(\frac{L}{T}\right)^l}. \quad (2.7)$$

In the tumor equation 2.1 ($\frac{dT}{dt}$), logistic growth ($aT(1 - bT)$) shows how the tumor grows naturally, while the terms $-cNT$ and $-DT$ show how N cells and CD8⁺T cells destroy tumor cells. The effect of chemotherapy is shown by $-K_T(1 - e^{-M})T$. The N cell equation 2.2 ($\frac{dN}{dt}$) includes how N cells are produced from circulating lymphocytes (eC), their natural death rate ($-fN$), how tumors cause them to grow ($g\frac{T^2}{h+T^2}N$), and how they become less effective after interacting with tumors ($-pNT$). Chemotherapy affects NK cells through $-K_N(1 - e^{-M})N$. The CD8⁺T cells equation 2.3 ($\frac{dL}{dt}$) includes several factors: natural death ($-mL$), how tumors recruit more CD8+ T cells ($j\frac{D^2T^2}{k+D^2T^2}L$), how tumor interactions make them exhausted ($-qLT$), how N and lymphocyte interactions help recruit them (r_1NT and r_2CT), how N cells regulate them ($-uNL^2$), chemotherapy effects ($-K_L(1 - e^{-M})L$), IL-2 stimulation ($\frac{pIL_I}{gI+I}$), and external TIL addition ($v_L(t)$). Circulating lymphocytes equation 2.4 ($\frac{dC}{dt}$) maintain balance by constant production (α), natural death (βC), and chemotherapy effects ($-K_C(1 - e^{-M})C$). Chemotherapy equation 2.5 ($\frac{dM}{dt}$) and immunotherapy equation 2.6 ($\frac{dI}{dt}$) are eliminated through first-order kinetics ($-\gamma M$ and $-\mu_I I$) with external inputs ($v_M(t)$ and $v_I(t)$). Equation 2.7, the fractional kill term D measures how well CD8⁺T cells work against tumor cells, showing how immune-tumor interactions change over time.

The system is governed by three inputs that are essential for optimizing treatment outcomes. These inputs are summarized as follows:

- $v_L(t)$: External source of TIL (tumor infiltration lymphocytes)
- $v_M(t)$: External administration of chemotherapy drug
- $v_I(t)$: External administration of immunotherapy drug (IL-2)

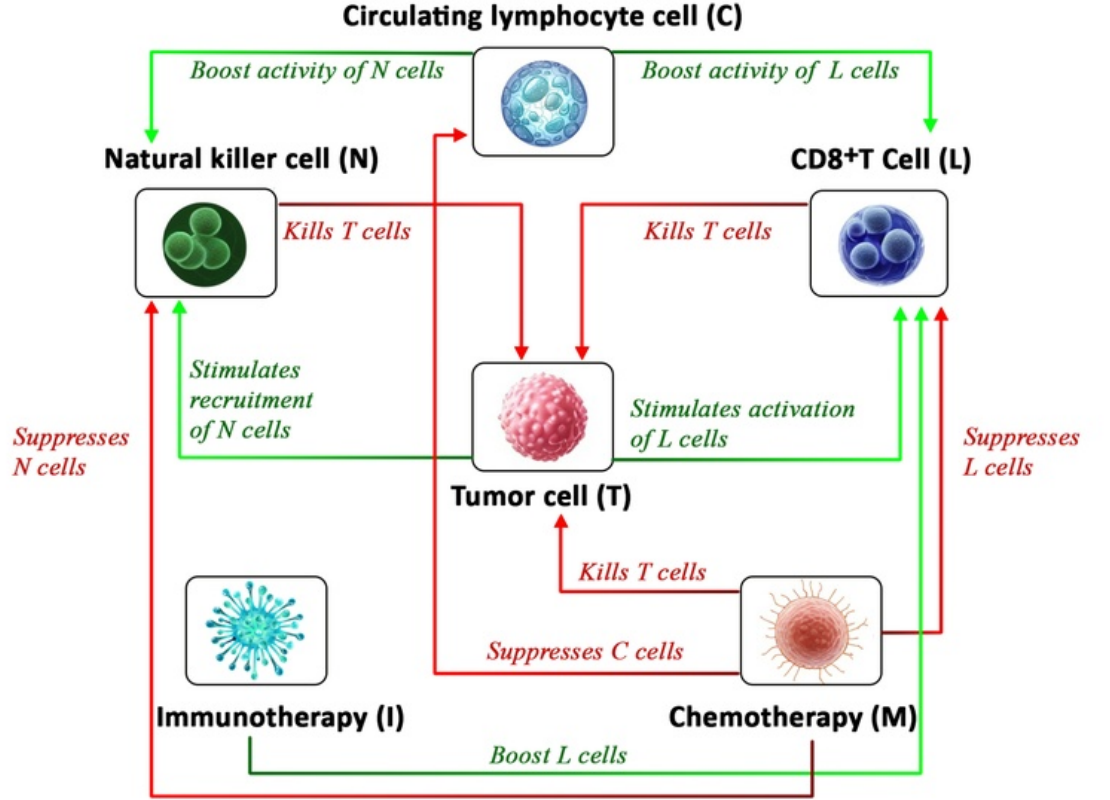


Figure 2.1: The schematic diagram depicts the interactions and effects of natural killer cells, $CD8^+$ T cells, circulating lymphocytes, chemotherapy, and immunotherapy on tumor cells.

Rewriting equation (2.1) - (2.7) by replacing $T(t)$, $N(t)$, $L(t)$, $C(t)$, $M(t)$ and $I(t)$ with x_1 , x_2 , x_3 , x_4 , x_5 and x_6 respectively, we get:

$$\dot{x}_1 = ax_1(1 - bx_1) - cx_2x_1 - Dx_1 - K_T(1 - e^{-x_5})x_1, \quad (2.8)$$

$$\dot{x}_2 = ex_4 - fx_2 + g\frac{x_1^2}{h+x_1^2}x_2 - px_2x_1 - K_N(1 - e^{-x_5})x_2, \quad (2.9)$$

$$\begin{aligned} \dot{x}_3 = & -mx_3 + j\frac{D^2x_1^2}{k+D^2x_1^2}x_3 - qx_3x_1 + (r_1x_2 + r_2x_4)x_1 \\ & - ux_2x_3^2 - K_L(1 - e^{-x_5})x_3 + \frac{pIx_3x_6}{g_I + x_6} + v_L(t), \end{aligned} \quad (2.10)$$

$$\dot{x}_4 = \alpha - \beta x_4 - K_C(1 - e^{-x_5})x_4, \quad (2.11)$$

$$\dot{x}_5 = -\gamma x_5 + v_M(t), \quad (2.12)$$

$$\dot{x}_6 = -\mu_I x_6 + v_I(t), \quad (2.13)$$

$$D = d\frac{\left(\frac{x_3}{x_1}\right)^l}{s + \left(\frac{x_3}{x_1}\right)^l}. \quad (2.14)$$

Table 2.1: HUMAN PARAMETER VALUES (PATIENT 9)

<i>No.</i>	<i>Symbol</i>	<i>Description</i>	<i>Value</i>	<i>Units</i>
1.	a	The growth rate of Tumor.	4.31×10^{-1}	day^{-1}
2.	b	$1/b$ is the tumor carrying capacity.	1.02×10^{-9}	cells^{-1}
3.	c	The fraction of tumor cells killed by NK cells.	6.41×10^{-11}	$\text{cells}^{-1} \text{day}^{-1}$
4.	d	The fraction of tumor cell killed by CD8+T cells.	2.34	day^{-1}
5.	e	The fraction of circulating lymphocytes becoming NK cells.	2.08×10^{-7}	day^{-1}
6.	l	Exponent of tumor cell in fraction which are killed by CD8+T cells.	2.09	None
7.	f	The death rate of NK cells.	4.12×10^{-2}	day^{-1}
8.	g	Maximum rate at which tumor cells recruit NK.	1.25×10^{-2}	day^{-1}
9.	h	The steepness coefficient of NK cells recruitment curve.	2.02×10^7	Cells^2
10.	j	Maximum recruitment rate of CD8+T cells.	2.49×10^{-2}	day^{-1}
11.	k	Steepness coefficient of the CD8+T cell recruitment curve.	3.66×10^7	Cell^2
12.	m	The death rate of CD8+T cells.	2.04×10^{-1}	day^{-1}
13.	q	Inactivation rate of CD8+T cells by tumor cells.	1.42×10^{-6}	$\text{cells}^{-1} \text{day}^{-1}$
14.	p	Inactivation rate of NK cells by Tumor cells.	3.42×10^{-6}	$\text{cells}^{-1} \text{day}^{-1}$
15.	s	Steepness coefficient of the Tumor and circulating lymphocyte interaction.	8.39×10^{-2}	None
16.	r_1	CD8+T cells production rate as a result of tumor cells killing by NK cells.	1.10×10^{-7}	$\text{cells}^{-1} \text{day}^{-1}$
17.	r_2	CD8+T cells production rate as a result of tumor cells killing by circulating lymphocytes.	6.50×10^{-11}	$\text{cells}^{-1} \text{day}^{-1}$
18.	u	NK cells regulatory function on CD8+T-cells.	3×10^{-10}	$\text{cells}^{-2} \text{day}^{-1}$
19.	k_T	The fraction of tumor cells killed by chemotherapy.	9×10^{-1}	day^{-1}
20.	k_N	The fraction of immune cells killed by chemotherapy	6×10^{-1}	day^{-1}
21.	k_L	The fraction of immune cells killed by chemotherapy.	6×10^{-1}	day^{-1}
22.	k_C	The fraction of immune cells killed by chemotherapy.	6×10^{-1}	day^{-1}
23.	α	Circulating lymphocytes source	7×10^8	$\text{cells}^{-1} \text{day}^{-1}$
24.	β	Natural death of circulating lymphocytes.	1×10^{-2}	day^{-1}
25.	γ	Chemotherapy drug decay rate.	9×10^{-1}	day^{-1}
26.	p_I	IL-2 recruitment rate of maximum CD8+T-cells.	1×10^{-1}	day^{-1}
27.	g_I	Steepness of recruitment curve of CD8+T-cells by IL-2.	2×10^7	Cell^2
28.	μ_I	The decay rate of IL-2 drug.	1×10^0	day^{-1}

Chapter 3

Controller Utilization And Methodology

This chapter discusses the use of advanced nonlinear robust control strategies, specifically TSMC, STSMC, ATSMC, and ASTSMC, to optimize drug dosages and treatment durations in mixed chemo-immunotherapy. The aim is to reduce toxicity and side effects while managing tumor growth and prioritizing patient health. Control gains are optimized using an Improved Grey Wolf Optimization algorithm, with the mean square error (MSE) as the objective function. A mathematical model is developed to combine these controllers for tumor reduction with minimal drug use and treatment time. The chapter details the designs of the controllers and reviews the various sliding mode control techniques that are applied. To ensure finite-time convergence of the tracking errors to their reference values, the controllers use sliding surfaces that define the desired system behavior. Since the immune system is regulated through external dosages in this model, the role of circulating lymphocytes (C) is considered negligible and is therefore not explicitly incorporated into the sliding surface formulation. This approach enables rapid tumor regression while minimizing side effects and maintaining patient stability, without adding unnecessary complexity into the control framework.

3.1 Robust Controller Design

In this section, robust control techniques TSMC and STSMC are discussed.

3.1.1 Terminal Sliding Mode Controller Design

The Terminal Sliding Mode Controller (TSMC) is a robust technique designed to make sure finite-time convergence of the system. By incorporating a nonlinear sliding surface, TSMC increases the system's ability to cope with uncertainties and disturbances, resulting in rapid error elimination and precise tracking performance. To enable the states to track their respective reference values, the tracking errors are defined as:

$$e_1 = x_1 - x_{1ref} \quad (3.1)$$

$$e_2 = x_2 - x_{2ref} \quad (3.2)$$

$$e_3 = x_3 - x_{3ref} \quad (3.3)$$

$$e_5 = x_5 - x_{5ref} \quad (3.4)$$

$$e_6 = x_6 - x_{6ref} \quad (3.5)$$

Where:

- e_1 : error between tumor cell population x_1 and its desired reference value x_{1ref} .
- e_2 : error between natural killer cell population x_2 and its desired reference value x_{2ref} .
- e_3 : error between CD8⁺ T cell population x_3 and its desired reference value x_{3ref} .
- e_5 : error between chemotherapy dose x_5 and its desired reference value x_{5ref} .
- e_6 : error between immunotherapy dose x_6 and its desired reference value x_{6ref} .

Additionally, the error $e_4 = x_4 - x_{4ref}$ represents the difference between the circulating lymphocyte population x_4 and its desired reference value x_{4ref} . While e_4 is not directly used in the sliding surface design, it is defined for completeness and reflects the behavior of x_4 within the system dynamics.

By taking the time derivative of the errors given in equations (3.1)-(3.5), we get

$$\dot{e}_1 = \dot{x}_1 - \dot{x}_{1ref} \quad (3.6)$$

$$\dot{e}_2 = \dot{x}_2 - \dot{x}_{2ref} \quad (3.7)$$

$$\dot{e}_3 = \dot{x}_3 - \dot{x}_{3ref} \quad (3.8)$$

$$\dot{e}_5 = \dot{x}_5 - \dot{x}_{5ref} \quad (3.9)$$

$$\dot{e}_6 = \dot{x}_6 - \dot{x}_{6ref} \quad (3.10)$$

We consider the three sliding surfaces as follows:

$$S_1 = c_1 e_1 + c_2 e_2 + c_3 e_3 + c_7 \left(\int e_1 dt \right)^{\frac{p_1}{q_1}} + c_8 \left(\int e_2 dt \right)^{\frac{p_2}{q_2}} + c_9 \left(\int e_3 dt \right)^{\frac{p_3}{q_3}} \quad (3.11)$$

$$S_2 = c_2 e_2 + c_5 e_5 + c_8 \left(\int e_2 dt \right)^{\frac{p_2}{q_2}} + c_{11} \left(\int e_5 dt \right)^{\frac{p_5}{q_5}} \quad (3.12)$$

$$S_3 = c_2 e_2 + c_6 e_6 + c_8 \left(\int e_2 dt \right)^{\frac{p_2}{q_2}} + c_{12} \left(\int e_6 dt \right)^{\frac{p_6}{q_6}} \quad (3.13)$$

Where:

- $c_1, c_2, c_3, c_5, c_6, c_7, c_8, c_9, c_{11}, c_{12}$ are design coefficients, and all are positive real numbers.
- p_1, p_2, p_3, p_5, p_6 and q_1, q_2, q_3, q_5, q_6 are positive odd integers such that $1 < \frac{p_i}{q_i} < 2$ for $i = 1, 2, 3, 5, 6$.

Taking time derivative of the sliding surfaces given in equations (3.11)-(3.13), we get

$$\begin{aligned} \dot{S}_1 = & c_1\dot{e}_1 + c_2\dot{e}_2 + c_3\dot{e}_3 + c_7e_1 \frac{p_1}{q_1} \left(\int e_1 dt \right)^{\frac{p_1}{q_1}-1} + \\ & c_8e_2 \frac{p_2}{q_2} \left(\int e_2 dt \right)^{\frac{p_2}{q_2}-1} + c_9e_3 \frac{p_3}{q_3} \left(\int e_3 dt \right)^{\frac{p_3}{q_3}-1} \end{aligned} \quad (3.14)$$

$$\dot{S}_2 = c_2\dot{e}_2 + c_5\dot{e}_5 + c_8e_2 \frac{p_2}{q_2} \left(\int e_2 dt \right)^{\frac{p_2}{q_2}-1} + c_{11}e_5 \frac{p_5}{q_5} \left(\int e_5 dt \right)^{\frac{p_5}{q_5}-1} \quad (3.15)$$

$$\dot{S}_3 = c_2\dot{e}_2 + c_6\dot{e}_6 + c_8e_2 \frac{p_2}{q_2} \left(\int e_2 dt \right)^{\frac{p_2}{q_2}-1} + c_{12}e_6 \frac{p_6}{q_6} \left(\int e_6 dt \right)^{\frac{p_6}{q_6}-1} \quad (3.16)$$

Substituting the values of \dot{e}_1 , \dot{e}_2 , \dot{e}_3 , \dot{e}_5 and \dot{e}_6 from equations (3.6)-(3.10) into equations (3.14)-(3.16), we get

$$\begin{aligned} \dot{S}_1 = & c_1(\dot{x}_1 - \dot{x}_{1ref}) + c_2(\dot{x}_2 - \dot{x}_{2ref}) + c_3(\dot{x}_3 - \dot{x}_{3ref}) + \\ & c_7e_1 \frac{p_1}{q_1} \left(\int e_1 dt \right)^{\frac{p_1}{q_1}-1} + c_8e_2 \frac{p_2}{q_2} \left(\int e_2 dt \right)^{\frac{p_2}{q_2}-1} + c_9e_3 \frac{p_3}{q_3} \left(\int e_3 dt \right)^{\frac{p_3}{q_3}-1} \end{aligned} \quad (3.17)$$

$$\begin{aligned} \dot{S}_2 = & c_2(\dot{x}_2 - \dot{x}_{2ref}) + c_5(\dot{x}_5 - \dot{x}_{5ref}) + c_8e_2 \frac{p_2}{q_2} \left(\int e_2 dt \right)^{\frac{p_2}{q_2}-1} + \\ & c_{11}e_5 \frac{p_5}{q_5} \left(\int e_5 dt \right)^{\frac{p_5}{q_5}-1} \end{aligned} \quad (3.18)$$

$$\begin{aligned} \dot{S}_3 = & c_2(\dot{x}_2 - \dot{x}_{2ref}) + c_6(\dot{x}_6 - \dot{x}_{6ref}) + c_8e_2 \frac{p_2}{q_2} \left(\int e_2 dt \right)^{\frac{p_2}{q_2}-1} + \\ & c_{12}e_6 \frac{p_6}{q_6} \left(\int e_6 dt \right)^{\frac{p_6}{q_6}-1} \end{aligned} \quad (3.19)$$

By substituting the values of \dot{x}_1 , \dot{x}_2 , \dot{x}_3 , \dot{x}_5 , and \dot{x}_6 from equations (2.8)-(2.13), into equations (3.17)-(3.19), we get

$$\begin{aligned}
\dot{S}_1 = & c_1 (ax_1(1 - bx_1) - cx_2x_1 - Dx_1 - k_T(1 - e^{-x_5})x_1 - \dot{x}_{1ref}) + \\
& c_2(ex_4 - fx_2 + g\frac{x_1^2}{h+x_1^2}x_2 - px_2x_1 - k_N(1 - e^{-x_5})x_2 - \dot{x}_{2ref}) + \\
& c_3(-mx_3 + j\frac{D^2x_1^2}{k+D^2x_1^2}x_3 - qx_3x_1 + (r_1x_2 + r_2x_4)x_1 \\
& - ux_2x_3^2 - k_L(1 - e^{-x_5})x_3 + \frac{p_Ix_3x_6}{g_I+x_6} + v_L(t) - \dot{x}_{3ref}) + \\
& c_7e_1\frac{p_1}{q_1}\left(\int e_1 dt\right)^{\frac{p_1}{q_1}-1} + c_8e_2\frac{p_2}{q_2}\left(\int e_2 dt\right)^{\frac{p_2}{q_2}-1} + \\
& c_9e_3\frac{p_3}{q_3}\left(\int e_3 dt\right)^{\frac{p_3}{q_3}-1}
\end{aligned} \tag{3.20}$$

$$\begin{aligned}
\dot{S}_2 = & c_2(ex_4 - fx_2 + g\frac{x_1^2}{h+x_1^2}x_2 - px_2x_1 - k_N(1 - e^{-x_5})x_2 - \dot{x}_{2ref}) \\
& + c_5(-\gamma x_5 + v_M(t) - \dot{x}_{5ref}) + c_8e_2\frac{p_2}{q_2}\left(\int e_2 dt\right)^{\frac{p_2}{q_2}-1} + \\
& c_{11}e_5\frac{p_5}{q_5}\left(\int e_5 dt\right)^{\frac{p_5}{q_5}-1}
\end{aligned} \tag{3.21}$$

$$\begin{aligned}
\dot{S}_3 = & c_2(ex_4 - fx_2 + g\frac{x_1^2}{h+x_1^2}x_2 - px_2x_1 - k_N(1 - e^{-x_5})x_2 - \dot{x}_{2ref}) \\
& + c_6(-\mu_Ix_6 + v_I(t) - \dot{x}_{6ref}) + c_8e_2\frac{p_2}{q_2}\left(\int e_2 dt\right)^{\frac{p_2}{q_2}-1} + \\
& c_{12}e_6\frac{p_6}{q_6}\left(\int e_6 dt\right)^{\frac{p_6}{q_6}-1}
\end{aligned} \tag{3.22}$$

To analyze the stability of the system, a Lyapunov candidate function is designed as:

$$V = \frac{1}{2}S_1^2 + \frac{1}{2}S_2^2 + \frac{1}{2}S_3^2 \tag{3.23}$$

Taking time derivative of equation (3.23), we get

$$\dot{V} = S_1\dot{S}_1 + S_2\dot{S}_2 + S_3\dot{S}_3 \tag{3.24}$$

Substitute the values of \dot{S}_1 , \dot{S}_2 , and \dot{S}_3 from equations (3.20) - (3.22), in equation 3.24, we get:

$$\begin{aligned}
\dot{V} = & S_1 \left(c_1 (ax_1(1 - bx_1) - cx_2x_1 - Dx_1 - k_T(1 - e^{-x_5})x_1 - \dot{x}_{1ref}) + \right. \\
& c_2(ex_4 - fx_2 + g\frac{x_1^2}{h+x_1^2}x_2 - px_2x_1 - k_N(1 - e^{-x_5})x_2 - \dot{x}_{2ref}) + \\
& c_3(-mx_3 + j\frac{D^2x_1^2}{k+D^2x_1^2}x_3 - qx_3x_1 + (r_1x_2 + r_2x_4)x_1 - ux_2x_3^2 - \\
& k_L(1 - e^{-x_5})x_3 + \frac{p_1x_3x_6}{g_1+x_6} + v_L(t) - \dot{x}_{3ref}) + c_7e_1\frac{p_1}{q_1} \left(\int e_1 dt \right)^{\frac{p_1}{q_1}-1} \\
& + c_8e_2\frac{p_2}{q_2} \left(\int e_2 dt \right)^{\frac{p_2}{q_2}-1} + c_9e_3\frac{p_3}{q_3} \left(\int e_3 dt \right)^{\frac{p_3}{q_3}-1} \left. \right) + S_2 \left(c_2(ex_4 \right. \\
& - fx_2 + g\frac{x_1^2}{h+x_1^2}x_2 - px_2x_1 - k_N(1 - e^{-x_5})x_2 - \dot{x}_{2ref}) + c_5(-\gamma x_5 \\
& + v_M(t) - \dot{x}_{5ref}) + c_8e_2\frac{p_2}{q_2} \left(\int e_2 dt \right)^{\frac{p_2}{q_2}-1} + c_{11}e_5\frac{p_5}{q_5} \left(\int e_5 dt \right)^{\frac{p_5}{q_5}-1} \left. \right) + \\
& S_3 \left(c_2(ex_4 - fx_2 + g\frac{x_1^2}{h+x_1^2}x_2 - px_2x_1 - k_N(1 - e^{-x_5})x_2 - \dot{x}_{2ref}) \right. \\
& + c_6(-\mu_1x_6 + v_I(t) - \dot{x}_{6ref}) + c_8e_2\frac{p_2}{q_2} \left(\int e_2 dt \right)^{\frac{p_2}{q_2}-1} + \\
& \left. + c_{12}e_6\frac{p_6}{q_6} \left(\int e_6 dt \right)^{\frac{p_6}{q_6}-1} \right) \tag{3.25}
\end{aligned}$$

By reaching law, we define the signum candid functions as:

$$\dot{S}_1 = -k_1|S_1|^\alpha \text{sign}(S_1) \tag{3.26}$$

$$\dot{S}_2 = -k_2|S_2|^\alpha \text{sign}(S_2) \tag{3.27}$$

$$\dot{S}_3 = -k_3|S_3|^\alpha \text{sign}(S_3) \tag{3.28}$$

Where

$$\text{sign}(S_n) = \begin{cases} 1, & \text{if } S_n > 0 \\ 0, & \text{if } S_n = 0 \\ -1, & \text{if } S_n < 0 \end{cases} \tag{3.29}$$

Where $n=1, 2, 3$ and k_1, k_2, k_3 and α are positive number, with α having a value between 0 and 1.

From equations (3.20)-(3.22) and equations (3.26)-(3.28), we get

$$\begin{aligned}
-k_1|S_1|^\alpha \text{sign}(S_1) = & c_1 (ax_1(1 - bx_1) - cx_2x_1 - Dx_1 - k_T(1 - e^{-x_5})x_1 - \dot{x}_{1ref}) + \\
& c_2(ex_4 - fx_2 + g\frac{x_1^2}{h+x_1^2}x_2 - px_2x_1 - k_N(1 - e^{-x_5})x_2 - \dot{x}_{2ref}) + \\
& c_3(-mx_3 + j\frac{D^2x_1^2}{k+D^2x_1^2}x_3 - qx_3x_1 + (r_1x_2 + r_2x_4)x_1 \\
& - ux_2x_3^2 - k_L(1 - e^{-x_5})x_3 + \frac{pIx_3x_6}{g_I+x_6} + v_L(t) - \dot{x}_{3ref}) + \\
& c_7e_1\frac{p_1}{q_1}\left(\int e_1 dt\right)^{\frac{p_1}{q_1}-1} + c_8e_2\frac{p_2}{q_2}\left(\int e_2 dt\right)^{\frac{p_2}{q_2}-1} + \\
& c_9e_3\frac{p_3}{q_3}\left(\int e_3 dt\right)^{\frac{p_3}{q_3}-1}
\end{aligned} \tag{3.30}$$

$$\begin{aligned}
-k_2|S_2|^\alpha \text{sign}(S_2) = & c_2(ex_4 - fx_2 + g\frac{x_1^2}{h+x_1^2}x_2 - px_2x_1 - k_N(1 - e^{-x_5})x_2 - \dot{x}_{2ref}) \\
& + c_5(-\gamma x_5 + v_M(t) - \dot{x}_{5ref}) + c_8e_2\frac{p_2}{q_2}\left(\int e_2 dt\right)^{\frac{p_2}{q_2}-1} + \\
& c_{11}e_5\frac{p_5}{q_5}\left(\int e_5 dt\right)^{\frac{p_5}{q_5}-1}
\end{aligned} \tag{3.31}$$

$$\begin{aligned}
-k_3|S_3|^\alpha \text{sign}(S_3) = & c_2(ex_4 - fx_2 + g\frac{x_1^2}{h+x_1^2}x_2 - px_2x_1 - k_N(1 - e^{-x_5})x_2 - \dot{x}_{2ref}) \\
& + c_6(-\mu_I x_6 + v_I(t) - \dot{x}_{6ref}) + c_8e_2\frac{p_2}{q_2}\left(\int e_2 dt\right)^{\frac{p_2}{q_2}-1} + \\
& + c_{12}e_6\frac{p_6}{q_6}\left(\int e_6 dt\right)^{\frac{p_6}{q_6}-1}
\end{aligned} \tag{3.32}$$

By solving and simplifying equations (3.30)-(3.32), we get our desired control inputs.

$$\begin{aligned}
v_L(t) = & \frac{1}{c_3} \left[-k_1 |S_1|^\alpha \text{sign}(S_1) - \left(c_1(ax_1(1-bx_1) - cx_2x_1 - Dx_1 - \right. \right. \\
& k_T(1-e^{-x_5})x_1) + c_2(ex_4 - fx_2 + g\frac{x_1^2}{h+x_1^2}x_2 - px_2x_1 - \\
& \left. \left. k_N(1-e^{-x_5})x_2 \right) + c_1\dot{x}_{1ref} + c_2\dot{x}_{2ref} + c_3\dot{x}_{3ref} \right. \\
& - \left(c_7e_1\frac{p_1}{q_1} \left(\int e_1 dt \right)^{\frac{p_1}{q_1}-1} + c_8e_2\frac{p_2}{q_2} \left(\int e_2 dt \right)^{\frac{p_2}{q_2}-1} \right. \\
& \left. \left. + c_9e_3\frac{p_3}{q_3} \left(\int e_3 dt \right)^{\frac{p_3}{q_3}-1} \right) \right] + mx_3 - j\frac{D^2x_1^2}{k+D^2x_1^2}x_3 \\
& + qx_3x_1 - (r_1x_2 + r_2x_4)x_1 + ux_2x_3^2 + K_L(1-e^{-x_5})x_3 \\
& - \frac{p_1x_3x_6}{g_I + x_6}
\end{aligned} \tag{3.33}$$

$$\begin{aligned}
v_M(t) = & \frac{1}{c_5} \left[-k_2 |S_2|^\alpha \text{sign}(S_2) - c_2 \left(ex_4 - fx_2 + g\frac{x_1^2}{h+x_1^2}x_2 - px_2x_1 - \right. \right. \\
& \left. \left. k_N(1-e^{-x_5})x_2 \right) + c_2\dot{x}_{2ref} + c_5\dot{x}_{5ref} - \left(c_8e_2\frac{p_2}{q_2} \left(\int e_2 dt \right)^{\frac{p_2}{q_2}-1} + \right. \right. \\
& \left. \left. c_{11}e_5\frac{p_5}{q_5} \left(\int e_5 dt \right)^{\frac{p_5}{q_5}-1} \right) \right] + \gamma x_5
\end{aligned} \tag{3.34}$$

$$\begin{aligned}
v_I(t) = & \frac{1}{c_6} \left[-k_3 |S_3|^\alpha \text{sign}(S_3) - c_2 \left(ex_4 - fx_2 + g\frac{x_1^2}{h+x_1^2}x_2 - px_2x_1 - \right. \right. \\
& \left. \left. k_N(1-e^{-x_5})x_2 \right) + c_2\dot{x}_{2ref} + c_6\dot{x}_{6ref} - \left(c_8e_2\frac{p_2}{q_2} \left(\int e_2 dt \right)^{\frac{p_2}{q_2}-1} \right. \right. \\
& \left. \left. + c_{12}e_6\frac{p_6}{q_6} \left(\int e_6 dt \right)^{\frac{p_6}{q_6}-1} \right) \right] + \mu_I x_6
\end{aligned} \tag{3.35}$$

For stability analysis, substitute the values of \dot{S}_1 , \dot{S}_2 , and \dot{S}_3 from equations (3.26)-(3.28) in equation (3.24), we get

$$\dot{V} = S_1(-k_1|S_1|^\alpha \text{sign}(S_1)) + S_2(-k_2|S_2|^\alpha \text{sign}(S_2)) + S_3(-k_3|S_3|^\alpha \text{sign}(S_3))$$

$$\dot{V} = - \sum_{n=1}^3 S_n(k_n|S_n|^\alpha \text{sign}(S_n)) \tag{3.36}$$

From equation (3.36), Lyapunov analysis shows that \dot{V} is negative definite, which implies that the system is asymptotically stable.

3.1.2 Super Twisting Sliding Mode Controller Design

Super-twisting sliding mode control (STSMC) is another sophisticated robust control technique for controlling systems more effectively. A key advantage of STSMC lies in its ability to handle system uncertainties, external disturbances, and nonlinear behavior. It reduces the chattering phenomenon while ensuring finite-time convergence of the system. To ensure accurate tracking of states to their respective reference values, errors are defined as

$$e_1 = x_1 - x_{1ref} \quad (3.37)$$

$$e_2 = x_2 - x_{2ref} \quad (3.38)$$

$$e_3 = x_3 - x_{3ref} \quad (3.39)$$

$$e_5 = x_5 - x_{5ref} \quad (3.40)$$

$$e_6 = x_6 - x_{6ref} \quad (3.41)$$

Where:

- e_1 : error between tumor cell population x_1 and its desired reference value x_{1ref} .
- e_2 : error between natural killer cell population x_2 and its desired reference value x_{2ref} .
- e_3 : error between CD8⁺ T cell population x_3 and its desired reference value x_{3ref} .
- e_5 : error between chemotherapy dose x_5 and its desired reference value x_{5ref} .
- e_6 : error between immunotherapy dose x_6 and its desired reference value x_{6ref} .

By taking the time derivative of the errors given in equations (3.37)-(3.41), we get

$$\dot{e}_1 = \dot{x}_1 - \dot{x}_{1ref} \quad (3.42)$$

$$\dot{e}_2 = \dot{x}_2 - \dot{x}_{2ref} \quad (3.43)$$

$$\dot{e}_3 = \dot{x}_3 - \dot{x}_{3ref} \quad (3.44)$$

$$\dot{e}_5 = \dot{x}_5 - \dot{x}_{5ref} \quad (3.45)$$

$$\dot{e}_6 = \dot{x}_6 - \dot{x}_{6ref} \quad (3.46)$$

Additionally, the error $e_4 = x_4 - x_{4ref}$ represents the difference between the circulating lymphocyte population x_4 and its desired reference value x_{4ref} . While e_4 is not directly used in the sliding surface design, it is defined for completeness and reflects the behavior of x_4 within the system dynamics. We consider the three sliding surfaces as follows:

$$S_1 = c_1 e_1 + c_2 e_2 + c_3 e_3 \quad (3.47)$$

$$S_2 = c_2 e_2 + c_5 e_5 \quad (3.48)$$

$$S_3 = c_2 e_2 + c_6 e_6 \quad (3.49)$$

Where c_1, c_2, c_3, c_5 and c_6 are real positive numbers.

Taking time derivative of equations (3.47)-(3.49) , we get

$$\dot{S}_1 = c_1\dot{e}_1 + c_2\dot{e}_2 + c_3\dot{e}_3 \quad (3.50)$$

$$\dot{S}_2 = c_2\dot{e}_2 + c_5\dot{e}_5 \quad (3.51)$$

$$\dot{S}_3 = c_2\dot{e}_2 + c_6\dot{e}_6 \quad (3.52)$$

Substituting the values of $\dot{e}_1, \dot{e}_2, \dot{e}_3, \dot{e}_5, \dot{e}_6$ from equations (3.42)-(3.46) in equations (3.50)-(3.52) , we get

$$\dot{S}_1 = c_1(\dot{x}_1 - \dot{x}_{1ref}) + c_2(\dot{x}_2 - \dot{x}_{2ref}) + c_3(\dot{x}_3 - \dot{x}_{3ref}) \quad (3.53)$$

$$\dot{S}_2 = c_2(\dot{x}_2 - \dot{x}_{2ref}) + c_5(\dot{x}_5 - \dot{x}_{5ref}) \quad (3.54)$$

$$\dot{S}_3 = c_2(\dot{x}_2 - \dot{x}_{2ref}) + c_6(\dot{x}_6 - \dot{x}_{6ref}) \quad (3.55)$$

Put the values of $\dot{x}_1, \dot{x}_2, \dot{x}_3, \dot{x}_5, \dot{x}_6$ from equations (2.8)-(2.14) into equations (3.53)-(3.55) , we get

$$\begin{aligned} \dot{S}_1 = & c_1 (ax_1(1 - bx_1) - cx_2x_1 - Dx_1 - k_T(1 - e^{-x_5})x_1 - \dot{x}_{1ref}) + \\ & c_2(ex_4 - fx_2 + g\frac{x_1^2}{h+x_1^2}x_2 - px_2x_1 - k_N(1 - e^{-x_5})x_2 - \dot{x}_{2ref}) + \\ & c_3(-mx_3 + j\frac{D^2x_1^2}{k+D^2x_1^2}x_3 - qx_3x_1 + (r_1x_2 + r_2x_4)x_1 \\ & - ux_2x_3^2 - k_L(1 - e^{-x_5})x_3 + \frac{p_Ix_3x_6}{g_I + x_6} + v_L(t) - \dot{x}_{3ref}) \end{aligned} \quad (3.56)$$

$$\begin{aligned} \dot{S}_2 = & c_2(ex_4 - fx_2 + g\frac{x_1^2}{h+x_1^2}x_2 - px_2x_1 - k_N(1 - e^{-x_5})x_2 - \dot{x}_{2ref}) \\ & + c_5(-\gamma x_5 + v_M(t) - \dot{x}_{5ref}) \end{aligned} \quad (3.57)$$

$$\begin{aligned} \dot{S}_3 = & c_2(ex_4 - fx_2 + g\frac{x_1^2}{h+x_1^2}x_2 - px_2x_1 - k_N(1 - e^{-x_5})x_2 - \dot{x}_{2ref}) \\ & + c_6(-\mu_I x_6 + v_I(t) - \dot{x}_{6ref}) \end{aligned} \quad (3.58)$$

To analyze the stability of the system, a Lyapunov candidate function is designed as:

$$V = \frac{1}{2}S_1^2 + \frac{1}{2}S_2^2 + \frac{1}{2}S_3^2 \quad (3.59)$$

Taking time derivative of equation (3.59), we get

$$\dot{V} = S_1\dot{S}_1 + S_2\dot{S}_2 + S_3\dot{S}_3 \quad (3.60)$$

Substitute the values of \dot{S}_1 , \dot{S}_2 , and \dot{S}_3 from equations (3.56)-(3.58) , in equation (3.60) , we get

$$\begin{aligned}
\dot{V} = & S_1 \left(c_1 (ax_1(1 - bx_1) - cx_2x_1 - Dx_1 - k_T(1 - e^{-x_5})x_1 - \dot{x}_{1ref}) + \right. \\
& c_2(ex_4 - fx_2 + g\frac{x_1^2}{h+x_1^2}x_2 - px_2x_1 - k_N(1 - e^{-x_5})x_2 - \dot{x}_{2ref}) + \\
& c_3(-mx_3 + j\frac{D^2x_1^2}{k+D^2x_1^2}x_3 - qx_3x_1 + (r_1x_2 + r_2x_4)x_1 - ux_2x_3^2 - \\
& k_L(1 - e^{-x_5})x_3 + \frac{p_Ix_3x_6}{g_I+x_6} + v_L(t) - \dot{x}_{3ref}) \left. \right) + S_2 \left(c_2(ex_4 \right. \\
& - fx_2 + g\frac{x_1^2}{h+x_1^2}x_2 - px_2x_1 - k_N(1 - e^{-x_5})x_2 - \dot{x}_{2ref}) + c_5(-\gamma x_5 \\
& + v_M(t) - \dot{x}_{5ref}) \left. \right) + S_3 \left(c_2(ex_4 - fx_2 + g\frac{x_1^2}{h+x_1^2}x_2 - px_2x_1 - \right. \\
& k_N(1 - e^{-x_5})x_2 - \dot{x}_{2ref}) + c_6(-\mu_Ix_6 + v_I(t) - \dot{x}_{6ref}) \left. \right) \tag{3.61}
\end{aligned}$$

Put $\dot{S}_1, \dot{S}_2, \dot{S}_3 = 0$ in equations (3.56)-(3.58) , we get

$$\begin{aligned}
0 = & c_1 (ax_1(1 - bx_1) - cx_2x_1 - Dx_1 - k_T(1 - e^{-x_5})x_1 - \dot{x}_{1ref}) + \\
& c_2(ex_4 - fx_2 + g\frac{x_1^2}{h+x_1^2}x_2 - px_2x_1 - k_N(1 - e^{-x_5})x_2 - \dot{x}_{2ref}) + \\
& c_3(-mx_3 + j\frac{D^2x_1^2}{k+D^2x_1^2}x_3 - qx_3x_1 + (r_1x_2 + r_2x_4)x_1 \\
& - ux_2x_3^2 - k_L(1 - e^{-x_5})x_3 + \frac{p_Ix_3x_6}{g_I+x_6} + v_L(t) - \dot{x}_{3ref}) \tag{3.62}
\end{aligned}$$

$$\begin{aligned}
0 = & c_2(ex_4 - fx_2 + g\frac{x_1^2}{h+x_1^2}x_2 - px_2x_1 - k_N(1 - e^{-x_5})x_2 - \dot{x}_{2ref}) \\
& + c_5(-\gamma x_5 + v_M(t) - \dot{x}_{5ref}) \tag{3.63}
\end{aligned}$$

$$\begin{aligned}
0 = & c_2(ex_4 - fx_2 + g\frac{x_1^2}{h+x_1^2}x_2 - px_2x_1 - k_N(1 - e^{-x_5})x_2 - \dot{x}_{2ref}) \\
& + c_6(-\mu_Ix_6 + v_I(t) - \dot{x}_{6ref}) \tag{3.64}
\end{aligned}$$

By solving and simplifying equations (3.62)-(3.64) , we get our equivalent control signals.

$$\begin{aligned}
u_{1eq} = & \frac{1}{c_3} \left[- \left(c_1 (ax_1 (1 - bx_1) - cx_2x_1 - Dx_1 - k_T (1 - e^{-x_5}) x_1) \right. \right. \\
& \left. \left. + c_2 (ex_4 - fx_2 + g \frac{x_1^2}{h + x_1^2} x_2 - px_2x_1 - k_N (1 - e^{-x_5}) x_2) \right) \right. \\
& \left. + c_1 \dot{x}_{1ref} + c_2 \dot{x}_{2ref} + c_3 \dot{x}_{3ref} \right] + mx_3 - j \frac{D^2 x_1^2}{k + D^2 x_1} x_3 + \\
& qx_3x_1 - (r_1x_2 + r_2x_4)x_1 + ux_2x_3^2 + K_L (1 - e^{-x_5}) x_3 - \frac{pIx_3x_6}{g_I + x_6}. \quad (3.65)
\end{aligned}$$

$$\begin{aligned}
u_{2eq} = & \frac{1}{c_5} \left[- c_2 \left(ex_4 - fx_2 + g \frac{x_1^2}{h + x_1^2} x_2 - px_2x_1 - k_N (1 - e^{-x_5}) x_2 \right) \right. \\
& \left. + c_2 \dot{x}_{2ref} + c_5 \dot{x}_{5ref} \right] + \gamma x_5 \quad (3.66)
\end{aligned}$$

$$\begin{aligned}
u_{3eq} = & \frac{1}{c_6} \left[- c_2 \left(ex_4 - fx_2 + g \frac{x_1^2}{h + x_1^2} x_2 - px_2x_1 - k_N (1 - e^{-x_5}) x_2 \right) \right. \\
& \left. + c_2 \dot{x}_{2ref} + c_6 \dot{x}_{6ref} \right] + \mu_I x_6 \quad (3.67)
\end{aligned}$$

For STSMC, the switching control is defined as:

$$u_{isw} = -k_i |S_i|^\alpha \text{sign}(S_i) - k_{ii} \int \text{sign}(S_i) dt \quad (3.68)$$

Where $i=1, 2, 3$ and k_i, k_{ii} , and α are positive constants, with α having a value between 0 and 1.

The final control law for STSMC is given as:

$$u_{iSTSMC} = u_{ieq} + u_{isw} \quad (3.69)$$

Where $i=1, 2, 3$.

By putting the values of u_{eq} and u_{sw} from equations (3.65)-(3.68) in equation (3.69), we get

$$\begin{aligned}
u_{1STSMC} = & \frac{1}{c_3} \left[- \left(c_1 (ax_1 (1 - bx_1) - cx_2x_1 - Dx_1 - k_T (1 - e^{-x_5}) x_1) \right. \right. \\
& \left. \left. + c_2 (ex_4 - fx_2 + g \frac{x_1^2}{h + x_1^2} x_2 - px_2x_1 - k_N (1 - e^{-x_5}) x_2) \right) \right. \\
& \left. + c_1 \dot{x}_{1ref} + c_2 \dot{x}_{2ref} + c_3 \dot{x}_{3ref} \right] + mx_3 - j \frac{D^2 x_1^2}{k + D^2 x_1} x_3 \\
& + qx_3x_1 - (r_1x_2 + r_2x_4) x_1 + ux_2x_3^2 + K_L (1 - e^{-x_5}) x_3 - \frac{pIx_3x_6}{gI + x_6} \\
& - k_1 |S_1|^{0.2} \text{sign}(S_1) - k_{11} \int \text{sign}(S_1) dt
\end{aligned} \tag{3.70}$$

$$\begin{aligned}
u_{2STSMC} = & \frac{1}{c_5} \left[- c_2 \left(ex_4 - fx_2 + g \frac{x_1^2}{h + x_1^2} x_2 - px_2x_1 - k_N (1 - e^{-x_5}) x_2 \right) \right. \\
& \left. + c_2 \dot{x}_{2ref} + c_5 \dot{x}_{5ref} \right] + \gamma x_5 - k_2 |S_2|^{0.2} \text{sign}(S_2) - \\
& k_{22} \int \text{sign}(S_2) dt
\end{aligned} \tag{3.71}$$

$$\begin{aligned}
u_{3STSMC} = & \frac{1}{c_6} \left[- c_2 \left(ex_4 - fx_2 + g \frac{x_1^2}{h + x_1^2} x_2 - px_2x_1 - k_N (1 - e^{-x_5}) x_2 \right) \right. \\
& \left. + c_2 \dot{x}_{2ref} + c_6 \dot{x}_{6ref} \right] + \mu x_6 - k_3 |S_3|^{0.2} \text{sign}(S_3) - \\
& k_{33} \int \text{sign}(S_3) dt
\end{aligned} \tag{3.72}$$

Using equations (3.70)-(3.72) and equation (3.61), we get

$$\dot{V} = - \sum_{n=1}^3 \left(S_n \left(k_n \text{sign}(S_n) + k_{nn} \int \text{sign}(S_n) dt \right) \right) \tag{3.73}$$

As \dot{V} is negative definite in equation (3.73), the system is stable and ensures finite-time convergence of all errors to zero.

3.2 Adaptive Controller Design

In this section, we design the ATSMC and ASTSMC using adaptive laws to get more accurate results.

3.2.1 Adaptive Terminal Sliding Mode Controller Design

To ensure the states track their respective reference values, the tracking errors are defined in equations (3.1)-(3.5) and the sliding surfaces are defined in equations (3.11)-(3.13).

We adapt the parameter g , as it varies between individuals and can be treated as an uncertain value. So let

$$\delta = g \quad (3.74)$$

For parameter estimation, we define the estimation error $\tilde{\delta}$ as:

$$\tilde{\delta} = \hat{\delta} - \delta \quad (3.75)$$

Where $\hat{\delta}$ is the estimated value of the parameter δ .

Putting $g = \delta$ in equations (3.20)-(3.22), we get

$$\begin{aligned} \dot{S}_1 = & c_1 (ax_1(1 - bx_1) - cx_2x_1 - Dx_1 - k_T(1 - e^{-x_5})x_1 - \dot{x}_{1ref}) + \\ & c_2(ex_4 - fx_2 + \delta \frac{x_1^2}{h + x_1^2}x_2 - px_2x_1 - k_N(1 - e^{-x_5})x_2 - \dot{x}_{2ref}) + \\ & c_3(-mx_3 + j \frac{D^2x_1^2}{k + D^2x_1^2}x_3 - qx_3x_1 + (r_1x_2 + r_2x_4)x_1 \\ & - ux_2x_3^2 - k_L(1 - e^{-x_5})x_3 + \frac{p_Ix_3x_6}{g_I + x_6} + v_L(t) - \dot{x}_{3ref}) + \\ & c_7e_1 \frac{p_1}{q_1} \left(\int e_1 dt \right)^{\frac{p_1}{q_1} - 1} + c_8e_2 \frac{p_2}{q_2} \left(\int e_2 dt \right)^{\frac{p_2}{q_2} - 1} + \\ & c_9e_3 \frac{p_3}{q_3} \left(\int e_3 dt \right)^{\frac{p_3}{q_3} - 1} \end{aligned} \quad (3.76)$$

$$\begin{aligned} \dot{S}_2 = & c_2(ex_4 - fx_2 + \delta \frac{x_1^2}{h + x_1^2}x_2 - px_2x_1 - k_N(1 - e^{-x_5})x_2 - \dot{x}_{2ref}) \\ & + c_5(-\gamma x_5 + v_M(t) - \dot{x}_{5ref}) + c_8e_2 \frac{p_2}{q_2} \left(\int e_2 dt \right)^{\frac{p_2}{q_2} - 1} + \\ & c_{11}e_5 \frac{p_5}{q_5} \left(\int e_5 dt \right)^{\frac{p_5}{q_5} - 1} \end{aligned} \quad (3.77)$$

$$\begin{aligned} \dot{S}_3 = & c_2(ex_4 - fx_2 + \delta \frac{x_1^2}{h + x_1^2}x_2 - px_2x_1 - k_N(1 - e^{-x_5})x_2 - \dot{x}_{2ref}) \\ & + c_6(-\mu_Ix_6 + v_I(t) - \dot{x}_{6ref}) + c_8e_2 \frac{p_2}{q_2} \left(\int e_2 dt \right)^{\frac{p_2}{q_2} - 1} + \\ & + c_{12}e_6 \frac{p_6}{q_6} \left(\int e_6 dt \right)^{\frac{p_6}{q_6} - 1} \end{aligned} \quad (3.78)$$

Using equations (3.75), the equations (3.76)-(3.78) becomes

$$\begin{aligned}
\dot{S}_1 = & c_1 (ax_1(1 - bx_1) - cx_2x_1 - Dx_1 - k_T(1 - e^{-x_5})x_1 - \dot{x}_{1ref}) + \\
& c_2(ex_4 - fx_2 + (\hat{\delta} - \tilde{\delta})\frac{x_1^2}{h+x_1^2}x_2 - px_2x_1 - k_N(1 - e^{-x_5})x_2 - \dot{x}_{2ref}) + \\
& c_3(-mx_3 + j\frac{D^2x_1^2}{k+D^2x_1^2}x_3 - qx_3x_1 + (r_1x_2 + r_2x_4)x_1 \\
& - ux_2x_3^2 - k_L(1 - e^{-x_5})x_3 + \frac{p_Ix_3x_6}{g_I+x_6} + v_L(t) - \dot{x}_{3ref}) + \\
& c_7e_1\frac{p_1}{q_1}\left(\int e_1 dt\right)^{\frac{p_1}{q_1}-1} + c_8e_2\frac{p_2}{q_2}\left(\int e_2 dt\right)^{\frac{p_2}{q_2}-1} + \\
& c_9e_3\frac{p_3}{q_3}\left(\int e_3 dt\right)^{\frac{p_3}{q_3}-1}
\end{aligned} \tag{3.79}$$

$$\begin{aligned}
\dot{S}_2 = & c_2(ex_4 - fx_2 + (\hat{\delta} - \tilde{\delta})\frac{x_1^2}{h+x_1^2}x_2 - px_2x_1 - k_N(1 - e^{-x_5})x_2 - \dot{x}_{2ref}) \\
& + c_5(-\gamma x_5 + v_M(t) - \dot{x}_{5ref}) + c_8e_2\frac{p_2}{q_2}\left(\int e_2 dt\right)^{\frac{p_2}{q_2}-1} + \\
& c_{11}e_5\frac{p_5}{q_5}\left(\int e_5 dt\right)^{\frac{p_5}{q_5}-1}
\end{aligned} \tag{3.80}$$

$$\begin{aligned}
\dot{S}_3 = & c_2(ex_4 - fx_2 + (\hat{\delta} - \tilde{\delta})\frac{x_1^2}{h+x_1^2}x_2 - px_2x_1 - k_N(1 - e^{-x_5})x_2 - \dot{x}_{2ref}) \\
& + c_6(-\mu_Ix_6 + v_I(t) - \dot{x}_{6ref}) + c_8e_2\frac{p_2}{q_2}\left(\int e_2 dt\right)^{\frac{p_2}{q_2}-1} + \\
& c_{12}e_6\frac{p_6}{q_6}\left(\int e_6 dt\right)^{\frac{p_6}{q_6}-1}
\end{aligned} \tag{3.81}$$

By separating $\tilde{\delta}$ from equations (3.79)-(3.81), we get

$$\begin{aligned}
\dot{S}_1 = & c_1 (ax_1(1 - bx_1) - cx_2x_1 - Dx_1 - k_T(1 - e^{-x_5})x_1 - \dot{x}_{1ref}) + \\
& c_2(ex_4 - fx_2 + \hat{\delta} \frac{x_1^2}{h + x_1^2}x_2 - px_2x_1 - k_N(1 - e^{-x_5})x_2 - \dot{x}_{2ref}) + \\
& c_3(-mx_3 + j \frac{D^2x_1^2}{k + D^2x_1^2}x_3 - qx_3x_1 + (r_1x_2 + r_2x_4)x_1 \\
& - ux_2x_3^2 - k_L(1 - e^{-x_5})x_3 + \frac{p_Ix_3x_6}{g_I + x_6} + v_L(t) - \dot{x}_{3ref}) + \\
& c_7e_1 \frac{p_1}{q_1} \left(\int e_1 dt \right)^{\frac{p_1}{q_1} - 1} + c_8e_2 \frac{p_2}{q_2} \left(\int e_2 dt \right)^{\frac{p_2}{q_2} - 1} + \\
& c_9e_3 \frac{p_3}{q_3} \left(\int e_3 dt \right)^{\frac{p_3}{q_3} - 1} - \tilde{\delta}c_2 \frac{x_1^2}{h + x_1^2}x_2
\end{aligned} \tag{3.82}$$

$$\begin{aligned}
\dot{S}_2 = & c_2(ex_4 - fx_2 + \hat{\delta} \frac{x_1^2}{h + x_1^2}x_2 - px_2x_1 - k_N(1 - e^{-x_5})x_2 - \dot{x}_{2ref}) \\
& + c_5(-\gamma x_5 + v_M(t) - \dot{x}_{5ref}) + c_8e_2 \frac{p_2}{q_2} \left(\int e_2 dt \right)^{\frac{p_2}{q_2} - 1} + \\
& c_{11}e_5 \frac{p_5}{q_5} \left(\int e_5 dt \right)^{\frac{p_5}{q_5} - 1} - \tilde{\delta}c_2 \frac{x_1^2}{h + x_1^2}x_2
\end{aligned} \tag{3.83}$$

$$\begin{aligned}
\dot{S}_3 = & c_2(ex_4 - fx_2 + \hat{\delta} \frac{x_1^2}{h + x_1^2}x_2 - px_2x_1 - k_N(1 - e^{-x_5})x_2 - \dot{x}_{2ref}) \\
& + c_6(-\mu_Ix_6 + v_I(t) - \dot{x}_{6ref}) + c_8e_2 \frac{p_2}{q_2} \left(\int e_2 dt \right)^{\frac{p_2}{q_2} - 1} + \\
& + c_{12}e_6 \frac{p_6}{q_6} \left(\int e_6 dt \right)^{\frac{p_6}{q_6} - 1} - \tilde{\delta}c_2 \frac{x_1^2}{h + x_1^2}x_2
\end{aligned} \tag{3.84}$$

For stability analysis, we consider the following positive definite Lyapunov candidate function:

$$V = \frac{1}{2}S_1^2 + \frac{1}{2}S_2^2 + \frac{1}{2}S_3^2 + \frac{1}{2\eta}\tilde{\delta}^2 \tag{3.85}$$

where η is a positive real number.

By computing the time derivative of V from equation (3.85), we get

$$\dot{V} = S_1\dot{S}_1 + S_2\dot{S}_2 + S_3\dot{S}_3 + \frac{1}{\eta}\tilde{\delta}\dot{\tilde{\delta}} \tag{3.86}$$

Now substitute the expressions of $\dot{S}_1, \dot{S}_2, \dot{S}_3$ from equations (3.82)-(3.84) in equation (3.86), we get

$$\begin{aligned}
\dot{V} = & S_1 \left(c_1 (ax_1(1 - bx_1) - cx_2x_1 - Dx_1 - k_T(1 - e^{-x_5})x_1 - \dot{x}_{1ref}) + \right. \\
& c_2(ex_4 - fx_2 + \hat{\delta} \frac{x_1^2}{h+x_1^2}x_2 - px_2x_1 - k_N(1 - e^{-x_5})x_2 - \dot{x}_{2ref}) + \\
& c_3(-mx_3 + j \frac{D^2x_1^2}{k+D^2x_1^2}x_3 - qx_3x_1 + (r_1x_2 + r_2x_4)x_1 - ux_2x_3^2 - \\
& k_L(1 - e^{-x_5})x_3 + \frac{p_Ix_3x_6}{g_I+x_6} + v_L(t) - \dot{x}_{3ref}) + c_7e_1 \frac{p_1}{q_1} \left(\int e_1 dt \right)^{\frac{p_1}{q_1}-1} \\
& + c_8e_2 \frac{p_2}{q_2} \left(\int e_2 dt \right)^{\frac{p_2}{q_2}-1} + c_9e_3 \frac{p_3}{q_3} \left(\int e_3 dt \right)^{\frac{p_3}{q_3}-1} - \tilde{\delta}c_2 \frac{x_1^2}{h+x_1^2}x_2 \Big) \\
& + S_2 \left(c_2(ex_4 - fx_2 + \hat{\delta} \frac{x_1^2}{h+x_1^2}x_2 - px_2x_1 - k_N(1 - e^{-x_5})x_2 - \dot{x}_{2ref}) \right. \\
& + c_5(-\gamma x_5 + v_M(t) - \dot{x}_{5ref}) + c_8e_2 \frac{p_2}{q_2} \left(\int e_2 dt \right)^{\frac{p_2}{q_2}-1} + \\
& c_{11}e_5 \frac{p_5}{q_5} \left(\int e_5 dt \right)^{\frac{p_5}{q_5}-1} - \tilde{\delta}c_2 \frac{x_1^2}{h+x_1^2}x_2 \Big) + S_3 \left(c_2(ex_4 - fx_2 \right. \\
& + \hat{\delta} \frac{x_1^2}{h+x_1^2}x_2 - px_2x_1 - k_N(1 - e^{-x_5})x_2 - \dot{x}_{2ref}) \\
& + c_6(-\mu_Ix_6 + v_I(t) - \dot{x}_{6ref}) + c_8e_2 \frac{p_2}{q_2} \left(\int e_2 dt \right)^{\frac{p_2}{q_2}-1} \\
& \left. + c_{12}e_6 \frac{p_6}{q_6} \left(\int e_6 dt \right)^{\frac{p_6}{q_6}-1} - \tilde{\delta}c_2 \frac{x_1^2}{h+x_1^2}x_2 \right) + \frac{1}{\eta} \tilde{\delta} \dot{\tilde{\delta}}
\end{aligned} \tag{3.87}$$

Taking $\tilde{\delta}$ common from equation (3.87), we get

$$\begin{aligned}
\dot{V} = & S_1 \left(c_1 (ax_1(1 - bx_1) - cx_2x_1 - Dx_1 - k_T(1 - e^{-x_5})x_1 - \dot{x}_{1ref}) + \right. \\
& c_2(ex_4 - fx_2 + \hat{\delta} \frac{x_1^2}{h + x_1^2} x_2 - px_2x_1 - k_N(1 - e^{-x_5})x_2 - \dot{x}_{2ref}) + \\
& c_3(-mx_3 + j \frac{D^2 x_1^2}{k + D^2 x_1^2} x_3 - qx_3x_1 + (r_1x_2 + r_2x_4)x_1 - ux_2x_3^2 - \\
& k_L(1 - e^{-x_5})x_3 + \frac{p_I x_3 x_6}{g_I + x_6} + v_L(t) - \dot{x}_{3ref}) + c_7 e_1 \frac{p_1}{q_1} \left(\int e_1 dt \right)^{\frac{p_1}{q_1} - 1} \\
& + c_8 e_2 \frac{p_2}{q_2} \left(\int e_2 dt \right)^{\frac{p_2}{q_2} - 1} + c_9 e_3 \frac{p_3}{q_3} \left(\int e_3 dt \right)^{\frac{p_3}{q_3} - 1} \\
& + S_2 \left(c_2(ex_4 - fx_2 + \hat{\delta} \frac{x_1^2}{h + x_1^2} x_2 - px_2x_1 - k_N(1 - e^{-x_5})x_2 - \dot{x}_{2ref}) \right. \\
& + c_5(-\gamma x_5 + v_M(t) - \dot{x}_{5ref}) + c_8 e_2 \frac{p_2}{q_2} \left(\int e_2 dt \right)^{\frac{p_2}{q_2} - 1} + \\
& c_{11} e_5 \frac{p_5}{q_5} \left(\int e_5 dt \right)^{\frac{p_5}{q_5} - 1} \left. \right) + S_3 \left(c_2(ex_4 - fx_2 + \hat{\delta} \frac{x_1^2}{h + x_1^2} x_2 - \right. \\
& px_2x_1 - k_N(1 - e^{-x_5})x_2 - \dot{x}_{2ref}) + c_6(-\mu_I x_6 + v_I(t) - \dot{x}_{6ref}) \\
& + c_8 e_2 \frac{p_2}{q_2} \left(\int e_2 dt \right)^{\frac{p_2}{q_2} - 1} + c_{12} e_6 \frac{p_6}{q_6} \left(\int e_6 dt \right)^{\frac{p_6}{q_6} - 1} \left. \right) + \\
& \tilde{\delta} \left(\frac{\dot{\hat{\delta}}}{\eta} - \sum_{i=1}^3 S_i c_2 \frac{x_1^2}{h + x_1^2} x_2 \right)
\end{aligned} \tag{3.88}$$

For parameter estimation, we define the adaptive law as:

$$\dot{\hat{\delta}} = \sum_{i=1}^3 \eta (S_i c_2 \frac{x_1^2}{h + x_1^2} x_2) \tag{3.89}$$

Put the value of $\hat{\delta}$ from equations (3.88)-(3.89), we get

$$\begin{aligned}
\dot{V} = & S_1 \left(c_1 (ax_1(1 - bx_1) - cx_2x_1 - Dx_1 - k_T(1 - e^{-x_5})x_1 - \dot{x}_{1ref}) + \right. \\
& c_2(ex_4 - fx_2 + \hat{\delta} \frac{x_1^2}{h + x_1^2}x_2 - px_2x_1 - k_N(1 - e^{-x_5})x_2 - \dot{x}_{2ref}) + \\
& c_3(-mx_3 + j \frac{D^2x_1^2}{k + D^2x_1^2}x_3 - qx_3x_1 + (r_1x_2 + r_2x_4)x_1 - ux_2x_3^2 - \\
& k_L(1 - e^{-x_5})x_3 + \frac{p_Ix_3x_6}{g_I + x_6} + v_L(t) - \dot{x}_{3ref}) + c_7e_1 \frac{p_1}{q_1} \left(\int e_1 dt \right)^{\frac{p_1}{q_1} - 1} \\
& + c_8e_2 \frac{p_2}{q_2} \left(\int e_2 dt \right)^{\frac{p_2}{q_2} - 1} + c_9e_3 \frac{p_3}{q_3} \left(\int e_3 dt \right)^{\frac{p_3}{q_3} - 1} \Big) \\
& + S_2 \left(c_2(ex_4 - fx_2 + \hat{\delta} \frac{x_1^2}{h + x_1^2}x_2 - px_2x_1 - k_N(1 - e^{-x_5})x_2 - \dot{x}_{2ref}) \right. \\
& + c_5(-\gamma x_5 + v_M(t) - \dot{x}_{5ref}) + c_8e_2 \frac{p_2}{q_2} \left(\int e_2 dt \right)^{\frac{p_2}{q_2} - 1} + \\
& c_{11}e_5 \frac{p_5}{q_5} \left(\int e_5 dt \right)^{\frac{p_5}{q_5} - 1} \Big) + S_3 \left(c_2(ex_4 - fx_2 + \hat{\delta} \frac{x_1^2}{h + x_1^2}x_2 - \right. \\
& px_2x_1 - k_N(1 - e^{-x_5})x_2 - \dot{x}_{2ref}) + c_6(-\mu_Ix_6 + v_I(t) - \dot{x}_{6ref}) \\
& \left. + c_8e_2 \frac{p_2}{q_2} \left(\int e_2 dt \right)^{\frac{p_2}{q_2} - 1} + c_{12}e_6 \frac{p_6}{q_6} \left(\int e_6 dt \right)^{\frac{p_6}{q_6} - 1} \right) \tag{3.90}
\end{aligned}$$

By reaching law defined in equations (3.26)-(3.29), we get

$$\begin{aligned}
-k_1|S_1|^\alpha \text{sign}(S_1) = & c_1 (ax_1(1 - bx_1) - cx_2x_1 - Dx_1 - k_T(1 - e^{-x_5})x_1 - \dot{x}_{1ref}) + \\
& c_2(ex_4 - fx_2 + \hat{\delta} \frac{x_1^2}{h + x_1^2}x_2 - px_2x_1 - k_N(1 - e^{-x_5})x_2 - \dot{x}_{2ref}) + \\
& c_3(-mx_3 + j \frac{D^2x_1^2}{k + D^2x_1^2}x_3 - qx_3x_1 + (r_1x_2 + r_2x_4)x_1 \\
& - ux_2x_3^2 - k_L(1 - e^{-x_5})x_3 + \frac{p_Ix_3x_6}{g_I + x_6} + v_L(t) - \dot{x}_{3ref}) + \\
& c_7e_1 \frac{p_1}{q_1} \left(\int e_1 dt \right)^{\frac{p_1}{q_1} - 1} + c_8e_2 \frac{p_2}{q_2} \left(\int e_2 dt \right)^{\frac{p_2}{q_2} - 1} + \\
& c_9e_3 \frac{p_3}{q_3} \left(\int e_3 dt \right)^{\frac{p_3}{q_3} - 1} \tag{3.91}
\end{aligned}$$

$$\begin{aligned}
-k_2|S_2|^\alpha \text{sign}(S_2) &= c_2(ex_4 - fx_2 + \hat{\delta} \frac{x_1^2}{h+x_1^2} x_2 - px_2x_1 - k_N(1 - e^{-x_5})x_2 - \dot{x}_{2ref}) \\
&\quad + c_5(-\gamma x_5 + v_M(t) - \dot{x}_{5ref}) + c_8 e_2 \frac{p_2}{q_2} \left(\int e_2 dt \right)^{\frac{p_2}{q_2}-1} + \\
&\quad c_{11} e_5 \frac{p_5}{q_5} \left(\int e_5 dt \right)^{\frac{p_5}{q_5}-1}
\end{aligned} \tag{3.92}$$

$$\begin{aligned}
-k_3|S_3|^\alpha \text{sign}(S_3) &= c_2(ex_4 - fx_2 + (\hat{\delta} \frac{x_1^2}{h+x_1^2} x_2 - px_2x_1 - k_N(1 - e^{-x_5})x_2 - \dot{x}_{2ref}) \\
&\quad + c_6(-\mu_I x_6 + v_I(t) - \dot{x}_{6ref}) + c_8 e_2 \frac{p_2}{q_2} \left(\int e_2 dt \right)^{\frac{p_2}{q_2}-1} + \\
&\quad c_{12} e_6 \frac{p_6}{q_6} \left(\int e_6 dt \right)^{\frac{p_6}{q_6}-1}
\end{aligned} \tag{3.93}$$

By simplifying equations (3.91)-(3.93), we obtain our desired input controls.

$$\begin{aligned}
v_L(t) &= \frac{1}{c_3} \left[-k_1|S_1|^\alpha \text{sign}(S_1) - \left(c_1(ax_1(1 - bx_1) - cx_2x_1 - Dx_1 - \right. \right. \\
&\quad k_T(1 - e^{-x_5})x_1) + c_2(ex_4 - fx_2 + \hat{\delta} \frac{x_1^2}{h+x_1^2} x_2 - px_2x_1 - \\
&\quad \left. \left. k_N(1 - e^{-x_5})x_2 \right) + c_1\dot{x}_{1ref} + c_2\dot{x}_{2ref} + c_3\dot{x}_{3ref} \right. \\
&\quad \left. - \left(c_7 e_1 \frac{p_1}{q_1} \left(\int e_1 dt \right)^{\frac{p_1}{q_1}-1} + c_8 e_2 \frac{p_2}{q_2} \left(\int e_2 dt \right)^{\frac{p_2}{q_2}-1} \right. \right. \\
&\quad \left. \left. + c_9 e_3 \frac{p_3}{q_3} \left(\int e_3 dt \right)^{\frac{p_3}{q_3}-1} \right) \right] + mx_3 - j \frac{D^2 x_1^2}{k + D^2 x_1^2} x_3 \\
&\quad + qx_3x_1 - (r_1x_2 + r_2x_4)x_1 + ux_2x_3^2 + k_L(1 - e^{-x_5})x_3 \\
&\quad - \frac{p_I x_3 x_6}{g_I + x_6}.
\end{aligned} \tag{3.94}$$

$$\begin{aligned}
v_M(t) &= \frac{1}{c_5} \left[-k_2|S_2|^\alpha \text{sign}(S_2) - c_2 \left(ex_4 - fx_2 + \hat{\delta} \frac{x_1^2}{h+x_1^2} x_2 - px_2x_1 - \right. \right. \\
&\quad \left. \left. k_N(1 - e^{-x_5})x_2 \right) + c_2\dot{x}_{2ref} + c_5\dot{x}_{5ref} - \left(c_8 e_2 \frac{p_2}{q_2} \left(\int e_2 dt \right)^{\frac{p_2}{q_2}-1} + \right. \right. \\
&\quad \left. \left. c_{11} e_5 \frac{p_5}{q_5} \left(\int e_5 dt \right)^{\frac{p_5}{q_5}-1} \right) \right] + \gamma x_5
\end{aligned} \tag{3.95}$$

$$\begin{aligned}
v_I(t) = & \frac{1}{c_6} \left[-k_3 |S_3|^\alpha \text{sign}(S_3) - c_2 \left(ex_4 - fx_2 + \hat{\delta} \frac{x_1^2}{h+x_1^2} x_2 - px_2x_1 - \right. \right. \\
& \left. \left. k_N (1 - e^{-x_5}) x_2 \right) + c_2 \dot{x}_{2ref} + c_6 \dot{x}_{6ref} - \left(c_8 e_2 \frac{p_2}{q_2} \left(\int e_2 dt \right)^{\frac{p_2}{q_2}-1} \right. \right. \\
& \left. \left. + c_{12} e_6 \frac{p_6}{q_6} \left(\int e_6 dt \right)^{\frac{p_6}{q_6}-1} \right) \right] + \mu_I x_6 \tag{3.96}
\end{aligned}$$

By substituting the updated values of \dot{S}_1 , \dot{S}_2 and \dot{S}_3 from equations (3.91)-(3.93) in equation (3.90), the Lyapunov function \dot{V} becomes:

$$\begin{aligned}
\dot{V} = & S_1(-k|S_1|^\alpha \text{sign}(S_1)) + S_2(-k_2|S_2|^\alpha \text{sign}(S_2)) + \\
& S_3(-k_3|S_3|^\alpha \text{sign}(S_3)) \tag{3.97}
\end{aligned}$$

$$\dot{V} = \sum_{i=1}^3 -k_i |S_i|^{\alpha+1} \text{sign}(S_i) \tag{3.98}$$

Hence, \dot{V} is negative definite, indicating that the overall system is asymptotically stable.

3.2.2 Adaptive Super Twisting Sliding Mode Controller Design

STSMC is adapted using an adaptive law to enhance robustness and reduce chattering. To ensure the states track their respective reference values, the tracking errors are defined in equations (3.1)-(3.5) and the sliding surfaces are defined in equations (3.47)-(3.49).

The parameter g , denoted as δ , is again adapted to address uncertainties and individual variations, with its estimation error $\tilde{\delta}$ specified in equations (3.74)-(3.75).

Putting $g = \delta$ in equations (3.56)-(3.58), we get

$$\begin{aligned}
\dot{S}_1 = & c_1 (ax_1(1 - bx_1) - cx_2x_1 - Dx_1 - k_T(1 - e^{-x_5})x_1 - \dot{x}_{1ref}) + \\
& + c_2(ex_4 - fx_2 + \delta \frac{x_1^2}{h + x_1^2}x_2 - px_2x_1 - k_N(1 - e^{-x_5})x_2 - \dot{x}_{2ref}) + \\
& c_3(-mx_3 + j \frac{D^2x_1^2}{k + D^2x_1^2}x_3 - qx_3x_1 + (r_1x_2 + r_2x_4)x_1 \\
& - ux_2x_3^2 - k_L(1 - e^{-x_5})x_3 + \frac{pIx_3x_6}{gI + x_6} + v_L(t) - \dot{x}_{3ref})
\end{aligned} \tag{3.99}$$

$$\begin{aligned}
\dot{S}_2 = & c_2(ex_4 - fx_2 + \delta \frac{x_1^2}{h + x_1^2}x_2 - px_2x_1 - k_N(1 - e^{-x_5})x_2 - \dot{x}_{2ref}) \\
& + c_5(-\gamma x_5 + v_M(t) - \dot{x}_{5ref})
\end{aligned} \tag{3.100}$$

$$\begin{aligned}
\dot{S}_3 = & c_2(ex_4 - fx_2 + \delta \frac{x_1^2}{h + x_1^2}x_2 - px_2x_1 - k_N(1 - e^{-x_5})x_2 - \dot{x}_{2ref}) \\
& + c_6(-\mu_I x_6 + v_I(t) - \dot{x}_{6ref})
\end{aligned} \tag{3.101}$$

Using equation (3.75), the equations (3.99)-(3.101) become

$$\begin{aligned}
\dot{S}_1 = & c_1 (ax_1(1 - bx_1) - cx_2x_1 - Dx_1 - k_T(1 - e^{-x_5})x_1 - \dot{x}_{1ref}) + \\
& c_2(ex_4 - fx_2 + (\hat{\delta} - \tilde{\delta}) \frac{x_1^2}{h + x_1^2}x_2 - px_2x_1 - k_N(1 - e^{-x_5})x_2 - \dot{x}_{2ref}) + \\
& c_3(-mx_3 + j \frac{D^2x_1^2}{k + D^2x_1^2}x_3 - qx_3x_1 + (r_1x_2 + r_2x_4)x_1 \\
& - ux_2x_3^2 - k_L(1 - e^{-x_5})x_3 + \frac{pIx_3x_6}{gI + x_6} + v_L(t) - \dot{x}_{3ref})
\end{aligned} \tag{3.102}$$

$$\begin{aligned}
\dot{S}_2 = & c_2(ex_4 - fx_2 + (\hat{\delta} - \tilde{\delta}) \frac{x_1^2}{h + x_1^2}x_2 - px_2x_1 - k_N(1 - e^{-x_5})x_2 - \dot{x}_{2ref}) \\
& + c_5(-\gamma x_5 + v_M(t) - \dot{x}_{5ref})
\end{aligned} \tag{3.103}$$

$$\begin{aligned}
\dot{S}_3 = & c_2(ex_4 - fx_2 + (\hat{\delta} - \tilde{\delta}) \frac{x_1^2}{h + x_1^2}x_2 - px_2x_1 - k_N(1 - e^{-x_5})x_2 - \dot{x}_{2ref}) \\
& + c_6(-\mu_I x_6 + v_I(t) - \dot{x}_{6ref})
\end{aligned} \tag{3.104}$$

By separating $\tilde{\delta}$ from equations (3.79)-(3.81), we get

$$\begin{aligned}
\dot{S}_1 = & c_1 (ax_1(1 - bx_1) - cx_2x_1 - Dx_1 - k_T(1 - e^{-x_5})x_1 - \dot{x}_{1ref}) + \\
& c_2(ex_4 - fx_2 + \hat{\delta} \frac{x_1^2}{h + x_1^2}x_2 - px_2x_1 - k_N(1 - e^{-x_5})x_2 - \dot{x}_{2ref}) + \\
& c_3(-mx_3 + j \frac{D^2x_1^2}{k + D^2x_1^2}x_3 - qx_3x_1 + (r_1x_2 + r_2x_4)x_1 \\
& - ux_2x_3^2 - k_L(1 - e^{-x_5})x_3 + \frac{PIx_3x_6}{g_I + x_6} + v_L(t) - \dot{x}_{3ref}) - \tilde{\delta}c_2 \frac{x_1^2}{h + x_1^2}x_2
\end{aligned} \tag{3.105}$$

$$\begin{aligned}
\dot{S}_2 = & c_2(ex_4 - fx_2 + \hat{\delta} \frac{x_1^2}{h + x_1^2}x_2 - px_2x_1 - k_N(1 - e^{-x_5})x_2 - \dot{x}_{2ref}) \\
& + c_5(-\gamma x_5 + v_M(t) - \dot{x}_{5ref}) - \tilde{\delta}c_2 \frac{x_1^2}{h + x_1^2}x_2
\end{aligned} \tag{3.106}$$

$$\begin{aligned}
\dot{S}_3 = & c_2(ex_4 - fx_2 + \hat{\delta} \frac{x_1^2}{h + x_1^2}x_2 - px_2x_1 - k_N(1 - e^{-x_5})x_2 - \dot{x}_{2ref}) \\
& + c_6(-\mu_I x_6 + v_I(t) - \dot{x}_{6ref}) - \tilde{\delta}c_2 \frac{x_1^2}{h + x_1^2}x_2
\end{aligned} \tag{3.107}$$

For stability analysis, we consider the following positive definite Lyapunov candidate function:

$$V = \frac{1}{2}S_1^2 + \frac{1}{2}S_2^2 + \frac{1}{2}S_3^2 + \frac{1}{2\eta} \tilde{\delta}^2 \tag{3.108}$$

where η is a positive real number.

By computing the time derivative of V from equations (3.85), we get

$$\dot{V} = S_1\dot{S}_1 + S_2\dot{S}_2 + S_3\dot{S}_3 + \frac{1}{\eta} \tilde{\delta} \dot{\tilde{\delta}} \tag{3.109}$$

Now substitute the expressions of $\dot{S}_1, \dot{S}_2, \dot{S}_3$ from equations (3.105)-(3.107) in equation (3.109), we get

$$\begin{aligned}
\dot{V} = & S_1 \left(c_1 (ax_1(1 - bx_1) - cx_2x_1 - Dx_1 - k_T(1 - e^{-x_5})x_1 - \dot{x}_{1ref}) + \right. \\
& c_2(ex_4 - fx_2 + \hat{\delta} \frac{x_1^2}{h + x_1^2} x_2 - px_2x_1 - k_N(1 - e^{-x_5})x_2 - \dot{x}_{2ref}) + \\
& c_3(-mx_3 + j \frac{D^2x_1^2}{k + D^2x_1^2} x_3 - qx_3x_1 + (r_1x_2 + r_2x_4)x_1 - ux_2x_3^2 - \\
& k_L(1 - e^{-x_5})x_3 + \frac{pIx_3x_6}{gI + x_6} + v_L(t) - \dot{x}_{3ref}) - \tilde{\delta} c_2 \frac{x_1^2}{h + x_1^2} x_2 \left. \right) \\
& + S_2 \left(c_2(ex_4 - fx_2 + \hat{\delta} \frac{x_1^2}{h + x_1^2} x_2 - px_2x_1 - k_N(1 - e^{-x_5})x_2 - \dot{x}_{2ref}) \right. \\
& + c_5(-\gamma x_5 + v_M(t) - \dot{x}_{5ref}) - \tilde{\delta} c_2 \frac{x_1^2}{h + x_1^2} x_2 \left. \right) + S_3 \left(c_2(ex_4 - fx_2 \right. \\
& + \hat{\delta} \frac{x_1^2}{h + x_1^2} x_2 - px_2x_1 - k_N(1 - e^{-x_5})x_2 - \dot{x}_{2ref}) \\
& + c_6(-\mu_I x_6 + v_I(t) - \dot{x}_{6ref}) - \tilde{\delta} c_2 \frac{x_1^2}{h + x_1^2} x_2 \left. \right) + \frac{1}{\eta} \tilde{\delta} \dot{\tilde{\delta}} \tag{3.110}
\end{aligned}$$

Taking $\tilde{\delta}$ common from equation (3.110), we get

$$\begin{aligned}
\dot{V} = & S_1 \left(c_1 (ax_1(1 - bx_1) - cx_2x_1 - Dx_1 - k_T(1 - e^{-x_5})x_1 - \dot{x}_{1ref}) + \right. \\
& c_2(ex_4 - fx_2 + \hat{\delta} \frac{x_1^2}{h + x_1^2} x_2 - px_2x_1 - k_N(1 - e^{-x_5})x_2 - \dot{x}_{2ref}) + \\
& c_3(-mx_3 + j \frac{D^2x_1^2}{k + D^2x_1^2} x_3 - qx_3x_1 + (r_1x_2 + r_2x_4)x_1 - ux_2x_3^2 - \\
& k_L(1 - e^{-x_5})x_3 + \frac{pIx_3x_6}{gI + x_6} + v_L(t) - \dot{x}_{3ref}) \left. \right) + S_2 \left(c_2(ex_4 - fx_2 \right. \\
& + \hat{\delta} \frac{x_1^2}{h + x_1^2} x_2 - px_2x_1 - k_N(1 - e^{-x_5})x_2 - \dot{x}_{2ref}) \\
& + c_5(-\gamma x_5 + v_M(t) - \dot{x}_{5ref}) \left. \right) + S_3 \left(c_2(ex_4 - fx_2 \right. \\
& + \hat{\delta} \frac{x_1^2}{h + x_1^2} x_2 - px_2x_1 - k_N(1 - e^{-x_5})x_2 - \dot{x}_{2ref}) \\
& + c_6(-\mu_I x_6 + v_I(t) - \dot{x}_{6ref}) \left. \right) + \tilde{\delta} \left(\frac{\dot{\tilde{\delta}}}{\eta} - \sum_{i=1}^3 S_i c_2 \frac{x_1^2}{h + x_1^2} x_2 \right) \tag{3.111}
\end{aligned}$$

For parameter estimation, we define the adaptive law as:

$$\hat{\delta} = \sum_{i=1}^3 \eta(S_i c_2 \frac{x_1^2}{h+x_1^2} x_2) \quad (3.112)$$

Put the value of $\hat{\delta}$ from equation (3.112) in equation (3.111), we get

$$\begin{aligned} \dot{V} = & S_1 \left(c_1 (ax_1(1-bx_1) - cx_2x_1 - Dx_1 - k_T(1-e^{-x_5})x_1 - \dot{x}_{1ref}) + \right. \\ & c_2(ex_4 - fx_2 + \hat{\delta} \frac{x_1^2}{h+x_1^2} x_2 - px_2x_1 - k_N(1-e^{-x_5})x_2 - \dot{x}_{2ref}) + \\ & c_3(-mx_3 + j \frac{D^2x_1^2}{k+D^2x_1^2} x_3 - qx_3x_1 + (r_1x_2 + r_2x_4)x_1 - ux_2x_3^2 - \\ & \left. k_L(1-e^{-x_5})x_3 + \frac{pIx_3x_6}{gI+x_6} + v_L(t) - \dot{x}_{3ref}) \right) + S_2 \left(c_2(ex_4 - fx_2 \right. \\ & \left. + \hat{\delta} \frac{x_1^2}{h+x_1^2} x_2 - px_2x_1 - k_N(1-e^{-x_5})x_2 - \dot{x}_{2ref}) \right. \\ & \left. + c_5(-\gamma x_5 + v_M(t) - \dot{x}_{5ref}) \right) + S_3 \left(c_2(ex_4 - fx_2 \right. \\ & \left. + \hat{\delta} \frac{x_1^2}{h+x_1^2} x_2 - px_2x_1 - k_N(1-e^{-x_5})x_2 - \dot{x}_{2ref}) \right. \\ & \left. + c_6(-\mu_I x_6 + v_I(t) - \dot{x}_{6ref}) \right) \end{aligned} \quad (3.113)$$

By putting the updated values of \dot{S}_1 , \dot{S}_2 , and \dot{S}_3 from equations (3.105)-(3.107) equal to zero, we get:

$$\begin{aligned} 0 = & c_1 (ax_1(1-bx_1) - cx_2x_1 - Dx_1 - k_T(1-e^{-x_5})x_1 - \dot{x}_{1ref}) + \\ & c_2(ex_4 - fx_2 + \hat{\delta} \frac{x_1^2}{h+x_1^2} x_2 - px_2x_1 - k_N(1-e^{-x_5})x_2 - \dot{x}_{2ref}) + \\ & c_3(-mx_3 + j \frac{D^2x_1^2}{k+D^2x_1^2} x_3 - qx_3x_1 + (r_1x_2 + r_2x_4)x_1 \\ & - ux_2x_3^2 - k_L(1-e^{-x_5})x_3 + \frac{pIx_3x_6}{gI+x_6} + v_L(t) - \dot{x}_{3ref}) \end{aligned} \quad (3.114)$$

$$\begin{aligned}
0 = & c_2(ex_4 - fx_2 + \hat{\delta} \frac{x_1^2}{h+x_1^2} x_2 - px_2x_1 - k_N(1 - e^{-x_5})x_2 - \dot{x}_{2ref}) \\
& + c_5(-\gamma x_5 + v_M(t) - \dot{x}_{5ref})
\end{aligned} \tag{3.115}$$

$$\begin{aligned}
0 = & c_2(ex_4 - fx_2 + \hat{\delta} \frac{x_1^2}{h+x_1^2} x_2 - px_2x_1 - k_N(1 - e^{-x_5})x_2 - \dot{x}_{2ref}) \\
& + c_6(-\mu_I x_6 + v_I(t) - \dot{x}_{6ref})
\end{aligned} \tag{3.116}$$

By solving and simplifying equations (3.114)-(3.116), we get our equivalent control signals.

$$\begin{aligned}
u_{1eq} = & \frac{1}{c_3} \left[- \left(c_1(ax_1(1 - bx_1) - cx_2x_1 - Dx_1 - k_T(1 - e^{-x_5})x_1) \right. \right. \\
& \left. \left. + c_2(ex_4 - fx_2 + \hat{\delta} \frac{x_1^2}{h+x_1^2} x_2 - px_2x_1 - k_N(1 - e^{-x_5})x_2) \right) \right. \\
& \left. + c_1\dot{x}_{1ref} + c_2\dot{x}_{2ref} + c_3\dot{x}_{3ref} \right] + mx_3 - j \frac{D^2x_1^2}{k + D^2x_1} x_3 + \\
& qx_3x_1 - (r_1x_2 + r_2x_4)x_1 + ux_2x_3^2 + K_L(1 - e^{-x_5})x_3 - \frac{pIx_3x_6}{g_I + x_6}
\end{aligned} \tag{3.117}$$

$$\begin{aligned}
u_{2eq} = & \frac{1}{c_5} \left[-c_2 \left(ex_4 - fx_2 + \hat{\delta} \frac{x_1^2}{h+x_1^2} x_2 - px_2x_1 - k_N(1 - e^{-x_5})x_2 \right) \right. \\
& \left. + c_2\dot{x}_{2ref} + c_5\dot{x}_{5ref} \right] + \gamma x_5
\end{aligned} \tag{3.118}$$

$$\begin{aligned}
u_{3eq} = & \frac{1}{c_6} \left[-c_2 \left(ex_4 - fx_2 + \hat{\delta} \frac{x_1^2}{h+x_1^2} x_2 - px_2x_1 - k_N(1 - e^{-x_5})x_2 \right) \right. \\
& \left. + c_2\dot{x}_{2ref} + c_6\dot{x}_{6ref} \right] + \mu_I x_6
\end{aligned} \tag{3.119}$$

For STSMC, the switching control is defined as:

$$u_{isw} = -k_i |S_i|^\alpha \text{sign}(S_i) - k_{ii} \int \text{sign}(S_i) dt \tag{3.120}$$

Where $i=1, 2, 3$ and k_i, k_{ii} , and α are positive constants, with α having a value between 0 and 1.

The final control law for STSMC is given as:

$$u_{iSTSMC} = u_{ieq} + u_{isw} \tag{3.121}$$

Where $i=1, 2, 3$.

By putting the values of u_{eq} and u_{sw} from equations (3.117)-(3.119) in equation (3.120), we get

$$\begin{aligned}
u_{1STSMC} = & \frac{1}{c_3} \left[- \left(c_1(ax_1(1-bx_1) - cx_2x_1 - Dx_1 - k_T(1-e^{-x_5})x_1) \right. \right. \\
& \left. \left. + c_2(ex_4 - fx_2 + \hat{\delta} \frac{x_1^2}{h+x_1^2}x_2 - px_2x_1 - k_N(1-e^{-x_5})x_2) \right) \right. \\
& \left. + c_1\dot{x}_{1ref} + c_2\dot{x}_{2ref} + c_3\dot{x}_{3ref} \right] + mx_3 - j \frac{D^2x_1^2}{k+D^2x_1}x_3 \\
& + qx_3x_1 - (r_1x_2 + r_2x_4)x_1 + ux_2x_3^2 + K_L(1-e^{-x_5})x_3 - \frac{pIx_3x_6}{gI+x_6} \\
& - k_1|S_1|^{0.2}sign(S_1) - k_{11} \int sign(S_1) dt
\end{aligned} \tag{3.122}$$

$$\begin{aligned}
u_{2STSMC} = & \frac{1}{c_5} \left[- c_2 \left(ex_4 - fx_2 + \hat{\delta} \frac{x_1^2}{h+x_1^2}x_2 - px_2x_1 - k_N(1-e^{-x_5})x_2 \right) \right. \\
& \left. + c_2\dot{x}_{2ref} + c_5\dot{x}_{5ref} \right] + \gamma x_5 - k_2|S_2|^{0.2}sign(S_2) - \\
& k_{22} \int sign(S_2) dt
\end{aligned} \tag{3.123}$$

$$\begin{aligned}
u_{3STSMC} = & \frac{1}{c_6} \left[- c_2 \left(ex_4 - fx_2 + \hat{\delta} \frac{x_1^2}{h+x_1^2}x_2 - px_2x_1 - k_N(1-e^{-x_5})x_2 \right) \right. \\
& \left. + c_2\dot{x}_{2ref} + c_6\dot{x}_{6ref} \right] + \mu_I x_6 - k_3|S_3|^{0.2}sign(S_3) - \\
& k_{33} \int sign(S_3) dt
\end{aligned} \tag{3.124}$$

Using equations (3.122)-(3.124) and equation (3.120), we get

$$\dot{V} = - \sum_{n=1}^3 \left(S_n \left(k_n sign(S_n) + k_{nn} \int sign(S_n) dt \right) \right) \tag{3.125}$$

As \dot{V} is negative definite in equation (3.73), the system is stable and ensures finite-time convergence of all errors to zero.

3.3 Controller Optimization

Improved Grey Wolf Optimization (IGWO) is a population-based algorithm inspired by the hunting behavior and social structure of grey wolves [14]. IGWO enhances the standard Grey Wolf Optimization (GWO) by introducing adaptive mechanisms and chaotic maps, which improve its ability to explore and exploit the search space. This helps the algorithm avoid getting stuck in local optima and speeds up convergence toward the global best

solution.

In IGWO, the wolf pack hierarchy consists of four search agents: alpha (α), beta (β), delta (δ), and omega (ω). The alpha agent represents the best solution, beta and delta represent the second and third-best solutions, and omega explores new areas randomly. This hierarchy allows IGWO to balance between exploring new solutions and improving existing ones.

In this study, IGWO is used to optimize the controller gains for four control strategies: Terminal Sliding Mode Controller (TSMC), Super-Twisting Sliding Mode Controller (STSMC), Adaptive Terminal Sliding Mode Controller (ATSMC), and Adaptive Super-Twisting Sliding Mode Controller (ASTSMC). The goal is to minimize the system error, evaluated using the Mean Squared Error (MSE) cost function. The MSE is defined as:

$$\min \text{MSE} = \min \left(\frac{1}{N} \sum_{i=1}^N (e_i)^2 \right) \quad (3.126)$$

where e_i is the error between the desired and actual output, and N is the total number of time steps or days in the simulation.

IGWO updates the search agents' positions in each iteration to reduce the MSE, leading to better controller performance. Figure (3.1) show the decreasing trend of the MSE cost function for each controller, proving IGWO's effectiveness in optimizing these control strategies.

The search process continues until a stopping condition is met, such as reaching the maximum number of iterations or achieving a predefined error level. The best solution is the search agent with the lowest MSE value.

Applying IGWO in this study successfully optimizes controller parameters, improving system stability and performance. The results demonstrate IGWO's flexibility and effectiveness in reducing the Mean Squared Error for different control systems.

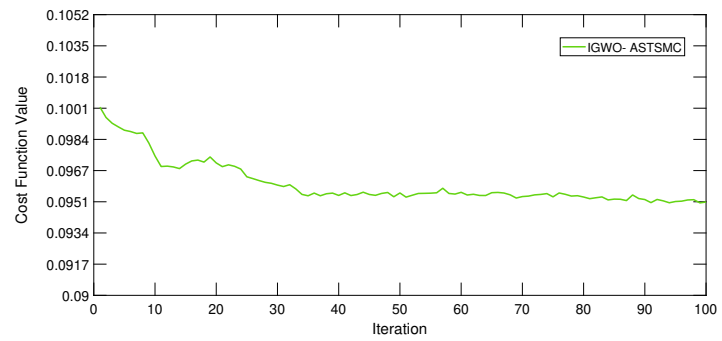
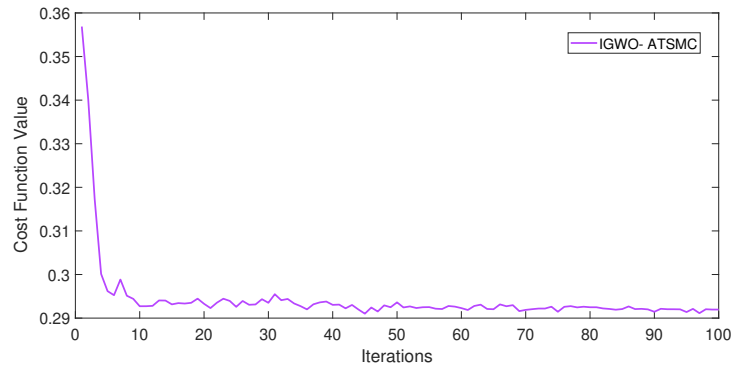
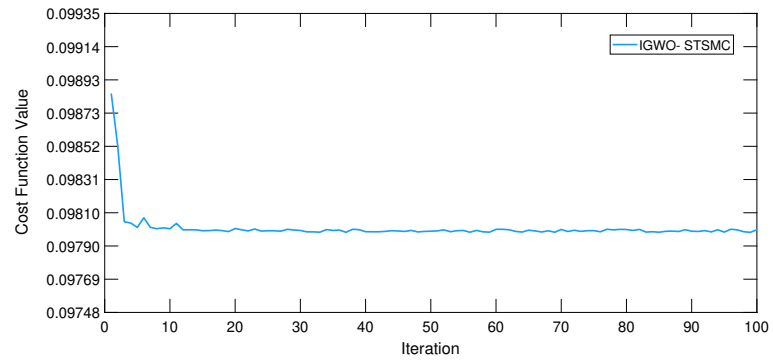
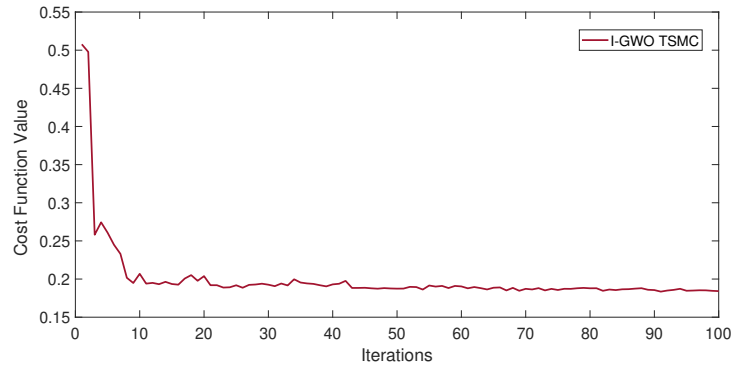


Figure 3.1: Decreasing Trend of MSE Cost Function for Different Controllers

Table 3.1 and Table 3.2 present the optimized controller gains, their corresponding values, and the cost values for the controllers.

Controller Gains	TSMC	ATSMC
c_1	0.505	63.101
c_2	103.694	0.145
c_3	0.245	0.100
c_5	4.642	7.214
c_6	13010	1706.7
c_7	1.552	1.000
c_8	0.004	1.0×10^{-6}
c_9	0.775	1.285
c_{11}	0.192	2.306
c_{12}	13010	1708.6
k_1	82.465	0.100
k_2	1.38×10^{-5}	1.3×10^{-5}
k_3	1.47×10^{-4}	0.546
Cost	0.1835	0.2910

Table 3.1: Optimized Gains and Costs for TSMC and ATSMC

Controller Gains	STSMC	ASTSMC
c_1	0.237	0.237
c_2	60.296	60.296
c_3	0.0011	0.001
c_5	0.179	0.0003
c_6	0.0001	0.0006
k_1	0.060	0.597
k_2	2.0×10^{-4}	1.0×10^{-4}
k_3	0.0010	1.0×10^{-4}
k_{11}	4.402	4.402
k_{22}	2.0×10^{-4}	1.0×10^{-4}
k_{33}	2.3×10^{-3}	4.0×10^{-4}
Cost	0.0979	0.0950

Table 3.2: Optimized Gains and Costs for STSMC and ASTSMC

Chapter 4

Results And Discussion

This chapter presents the simulation results and performance analysis of the proposed controllers applied to the cancer model described by equations (2.1)- (2.7).

MATLAB/SIMULINK was used to simulate tumor dynamics and evaluate the performance of the designed controllers.

The x-axis in all simulation graphs represents time (in days), while the y-axis represents the cell population. The comparison is done involving all four designed controllers and existing research.

In addition, the values of all the parameters used for the analysis are provided in Tables (2.1), (3.1), and (3.2). The initial conditions and drug dosage saturation (control bound) values used in this study are adopted from [24] and are presented in Tables 4.1 and 4.2.

Variable	Description	Initial Value
$T(0)$	Tumor Cell Population	2×10^7
$N(0)$	Natural Killer (NK) Cells	1×10^4
$L(0)$	CD8 ⁺ T Cells	100
$C(0)$	Circulating Lymphocytes	1×10^9
$M(0)$	Chemotherapy Concentration	0
$I(0)$	Immunotherapy Concentration	0

Table 4.1: Initial Conditions of States

Variable	Lower Limit	Upper Limit
$u_L(t)$ (cells day ⁻¹)	0	10^{10}
$u_M(t)$ (mg kg ⁻¹ day ⁻¹)	0	2
$u_I(t)$ (I.U. kg ⁻¹ day ⁻¹)	0	4×10^6

Table 4.2: Limits (Bounds) of Control Variables

4.1 Comparison of Robust Controllers

4.1.1 Tumor Cell Comparison

Figure 4.1 shows complete tumor regression under the four controllers: TSMC, STSMC, ATSMC, and ASTSMC. Among these, the ASTSMC demonstrates the remarkable performance, reducing the tumor population to 0.001 in just 9 days, owing to its high adaptability and precise control. The ATSMC follows closely, lowering the tumor to 0.002 in 10 days, reflecting its ability to handle system changes well. The STSMC achieves the same tumor reduction of 0.001 in 12 days, indicating moderate performance. In contrast, the TSMC is the slowest, taking 13 days to reach the same level. This comparison clearly shows the superiority of adaptive controllers, particularly the ASTSMC, in achieving rapid and stable tumor regression, making it a more robust and advantageous strategy for successful cancer treatment.

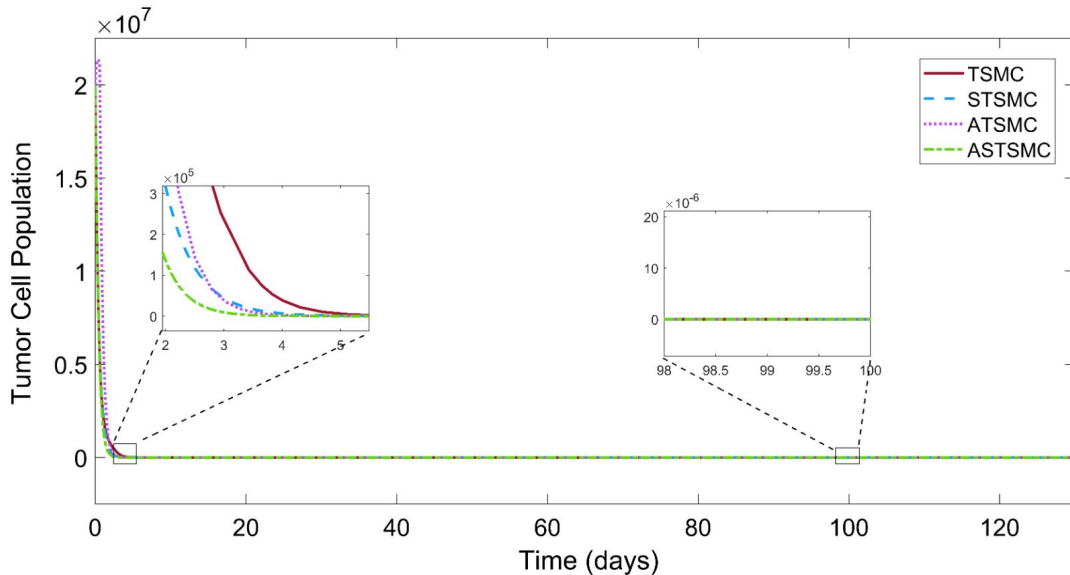


Figure 4.1: Tumor Cell Population Comparison Over Time.

4.1.2 Natural Killer Cell Comparison

Figure 4.2 demonstrates that all controllers stimulate natural killer cells (N) over time, eventually reaching a steady-state equilibrium. Initially, the presence of tumor cells and chemotherapy suppresses the N cell population. As the tumor burden and chemotherapy are reduced or eliminated, the N cells recover and achieve reference convergence in 800 days, reflecting the restoration of a healthy and functional immune system.

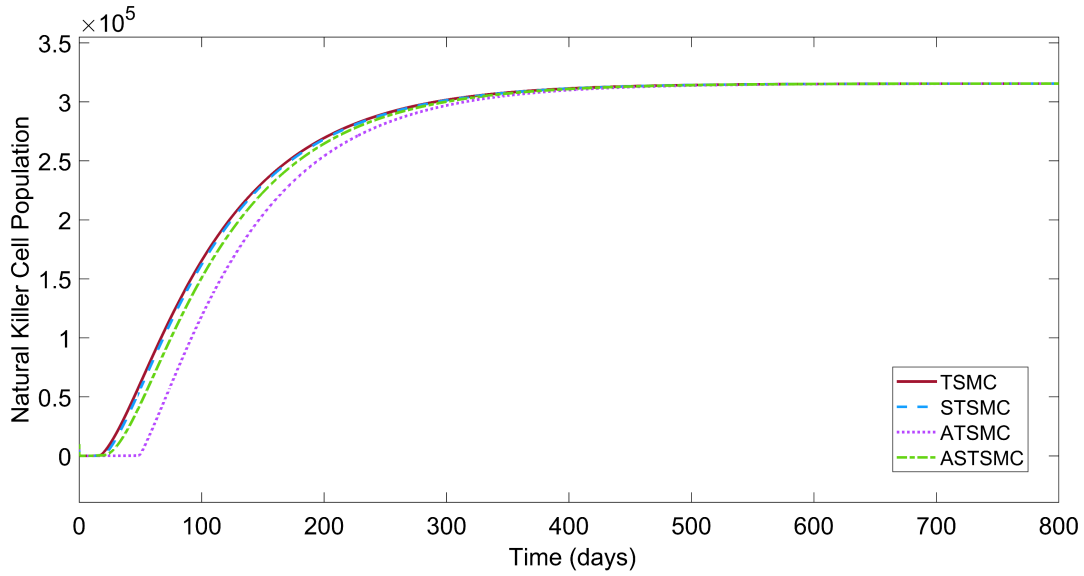


Figure 4.2: Natural Killer Cell Population Comparison Over Time.

4.1.3 CD8⁺ T Cell Comparison

Figure 4.17 illustrates the L cells dynamics under the controllers. At the start, all controllers exhibit an initial spike in L , representing the immune system's immediate response to the tumor presence and therapeutic interventions (TIL and IL-2). As the tumor burden decreases, the L population declines at varying rates. The TSMC achieves the fastest decay, with L reaching 0.01 within 80 days, reflecting its focus on rapid immune response suppression. The ATSMC follows, reaching 0.01 in 85 days, balancing control and maintaining the immune response slightly longer. The STSMC extends this duration further, with L reaching 0.01 in 100 days, showcasing moderate adaptability. The ASTSMC sustains L at higher levels for the longest time, with L reaching 0.01 only after 105 days, demonstrating its superior ability to sustain an immune response. This prolonged stimulation provided by ASTSMC is due to its highly adaptive design, which dynamically adjusts the immune system's response as needed. This helps maintain the immune response for a longer period, offering long-term benefits and reducing the risk of tumor relapse. These results shows that ASTSMC in maintaining a strong and lasting immune response during and after therapy.

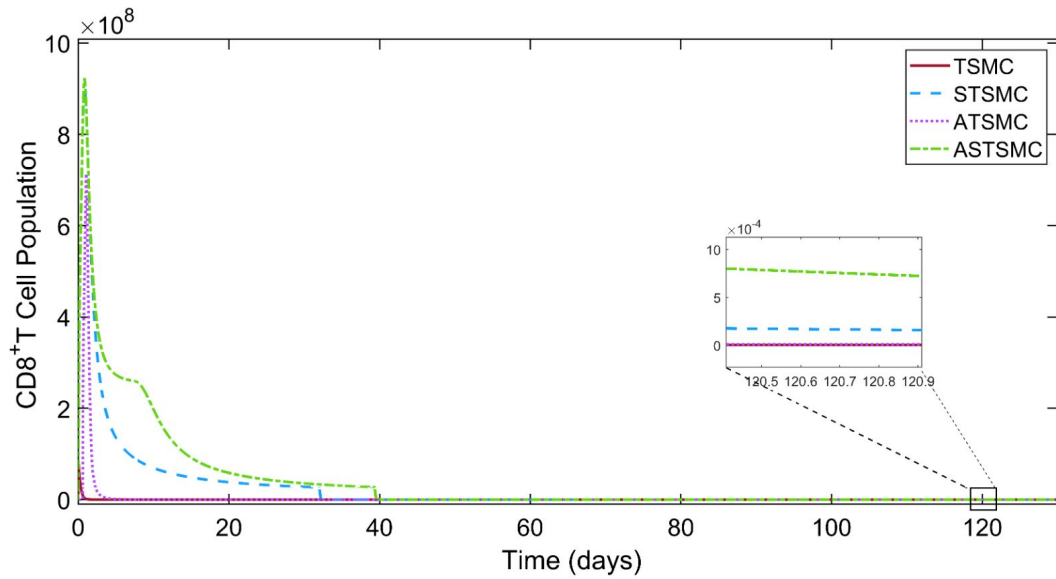


Figure 4.3: CD8⁺ T Cell Population Comparison Over Time.

4.1.4 Circulating Lymphocytes Comparison

Figure 4.4 displays the behavior of the C cells over time under the controllers. Initially, the presence of tumor cells and the effects of chemotherapy suppress the C population. However, during the treatment phase, C does not drop below 10^9 , ensuring that the immune system remains stable despite the therapeutic stress. For a healthy patient, C levels below 10^8 are considered unsafe, which confirms that the patient remains in a healthy state throughout the treatment. After the tumor burden decreases and chemotherapy is stopped, the C population gains strength, eventually achieving a reference convergence of order 10^{10} in 800 days. This reflects the full restoration of a healthy and functional immune system.

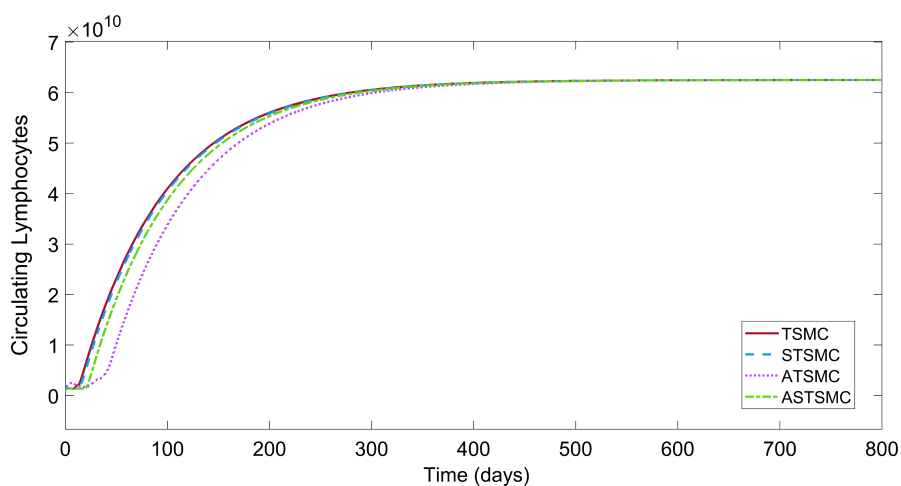


Figure 4.4: Circulating Lymphocytes Population Comparison Over Time.

4.1.5 Chemotherapy Concentration Comparison

Figure 4.5 depicts the behavior of chemotherapy drug concentration (M) under the controllers. At the start of treatment, M rises quickly due to the initial administration of the chemotherapy drug (v_M) to suppress the tumor. As the tumor decreases, M naturally declines because the body eliminates the drug faster than it is being administered.

TSMC and STSMC reduce M the fastest, bringing it down to 0.001 in 7 days. ATSMC takes 14 days, allowing M to decrease more slowly, while ASTSMC sustains M for the longest time, reaching 0.001 in 16 days. This shows that ASTSMC can extend the chemotherapy treatment when necessary. Throughout the treatment, the C cell population remains above 10^9 , ensuring no significant toxicity. By the end of the treatment, all controllers reduce M to zero, ensuring the complete elimination of chemotherapy from the body. These results provide insights into how the controllers successfully manage tumor suppression while ensuring patient safety.

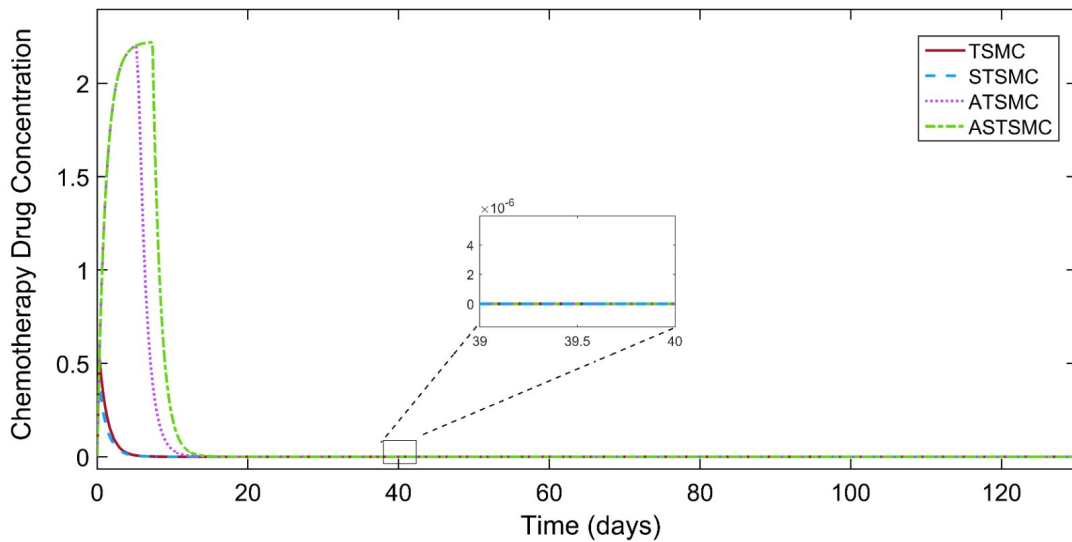


Figure 4.5: Chemotherapy Concentration Comparison Over Time.

4.1.6 Immunotherapy Concentration Comparison

Figure 4.6 shows the dynamics of the immunotherapy drug concentration (I) under the four controllers, which is influenced by v_I (IL-2). At the start of treatment, v_I is administered to stimulate the immune system, boosting the immune response. Each controller regulates v_I differently, leading to varying rates of decline in I .

TSMC reduces I to 0.01 within 4 days, reflecting a rapid decrease in immunotherapy concentration. STSMC achieves an even faster reduction, lowering I to 0.005 in just 2 days. ATSMC sustains immunotherapy longer, bringing I down to 0.003 over 10 days. ASTSMC completely phases out immunotherapy, reducing I to 0 in 10 days.

These results show how the controllers regulate immunotherapy to balance effective immune stimulation with the timely elimination of the drug. By the end of treatment, I is fully eliminated, ensuring no risk of overstimulation or adverse effects.

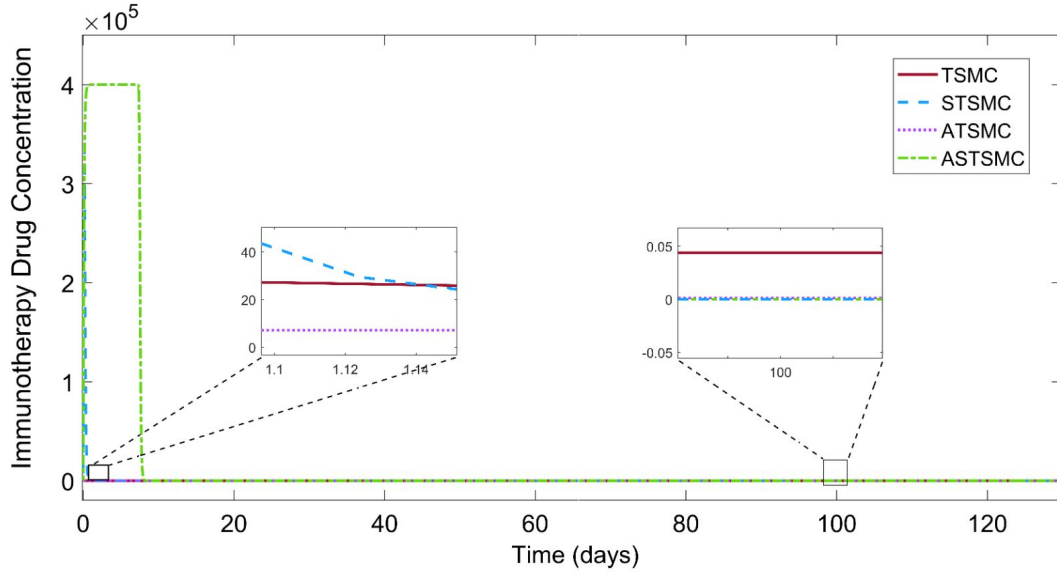
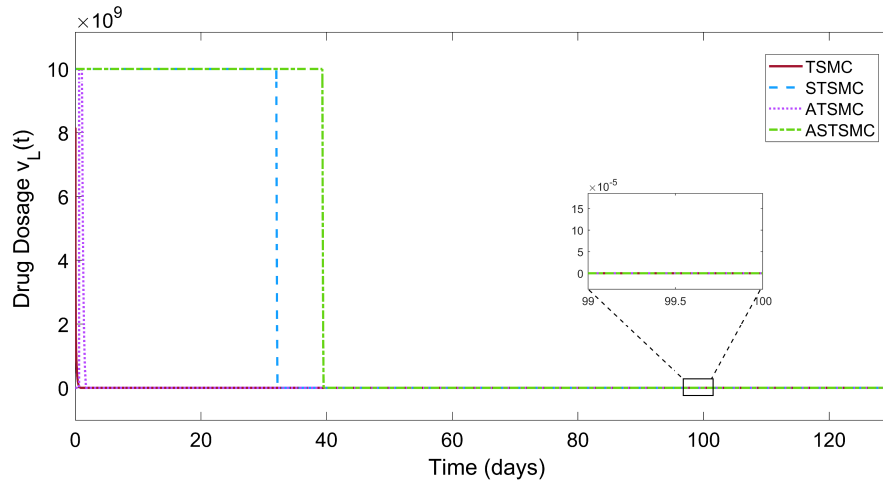


Figure 4.6: Immunotherapy Concentration Comparison Over Time.

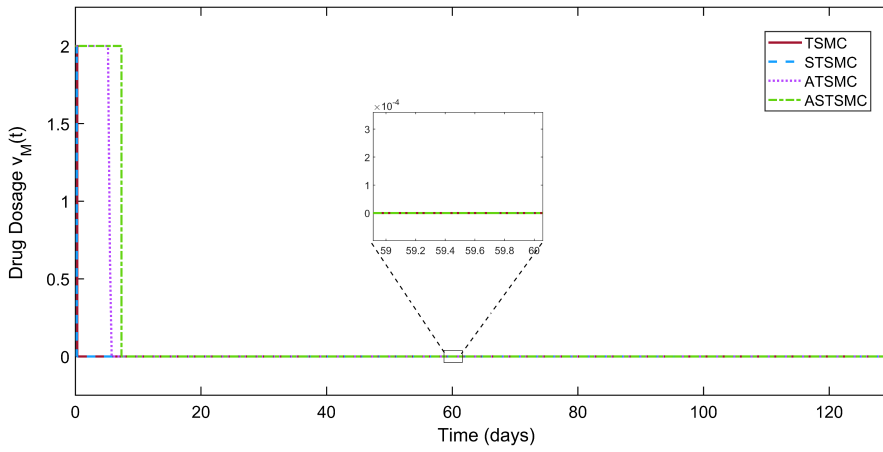
4.1.7 Drug Delivery Scenario

In this study, three types of drug dosages are considered (Figure 4.7): immunotherapy drug dosage (TIL): $v_L(t)$, immunotherapy drug dosage (IL-2): $v_I(t)$, and chemotherapy drug dosage: $v_m(t)$. Each drug dosage is regulated by the controllers such as TSMC, STSMC, ATSMC, and ASTSMC in order to achieve effective tumor suppression while ensuring therapy remains safe and within acceptable limits. The dynamics of drug elimination vary depending on the controller.

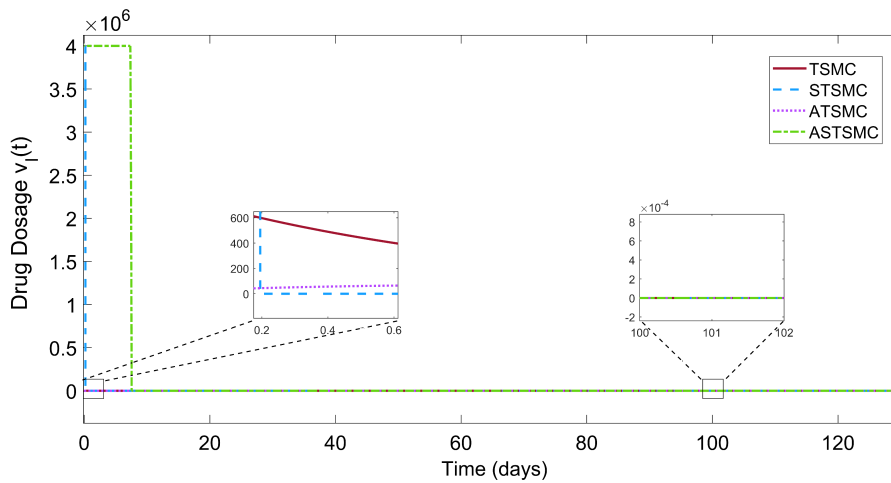
Under TSMC, $v_L(t)$, $v_m(t)$, and $v_I(t)$ are eliminated the fastest, reaching zero in 1 day, 0.3 days, and 3.6 days, respectively. STSMC phases out $v_L(t)$, $v_m(t)$, and $v_I(t)$ in 32 days, 0.2 days, and 0.2 days, respectively, showing a quicker reduction of chemotherapy and IL-2 but a slower elimination of TIL. ATSMC maintains the dosages slightly longer, reducing $v_L(t)$, $v_m(t)$, and $v_I(t)$ to zero in 1.7 days, 5.8 days, and 9.3 days, respectively. ASTSMC demonstrates the most extended duration of drug delivery, phasing out $v_L(t)$, $v_m(t)$, and $v_I(t)$ in 39 days, 7.3 days, and 7.5 days, respectively. These results show how the controllers handle drug delivery differently, ensuring the tumor is effectively treated while safely eliminating the drugs to avoid side effects.



(a)



(b)



(c)

Figure 4.7: Comparison of Drug Delivery Scenarios Across Controllers.

As shown in Table 4.3, the ASTSMC controller demonstrates the best overall perfor-

State	TSMC	STSMC	ATSMC	ASTSMC	Previous Study [24]
T	13	12	10	9	48.77
N	800	800	800	800	800
L	80	100	85	105	105.2
C	800	800	800	800	800
M	7	7	14	16	40.96
I	4	2	10	10	38.69

Table 4.3: Convergence of States (in Days) Under Different Controllers

mance in terms of convergence across all states. It achieves tumor regression in just 9 days, the fastest among the four controllers and significantly quicker than the 48.77 days reported in the previous study [24]. For chemotherapy drug clearance, ASTSMC requires 16 days, slightly longer than the TSMC and STSMC, but this allows it to sustain a controlled and gradual treatment process. Additionally, ASTSMC maintains immune cells at safe levels over time, providing a robust and adaptive approach for long-term therapy. The overall comparison indicates that ASTSMC is the most efficient and adaptive controller for tumor regression and immune system recovery.

4.2 Hardware-in-loop

Hardware-in-Loop (HIL) testing is used to test the performance of the proposed control strategies in real-time [4]. It is an affordable method where the system is converted into a discrete form to run in real-time, simulating real-world conditions. The setup, shown in Figure 4.8, uses a Delfino C2000 LaunchPad F28379D integrated with MATLAB/Simulink. The results confirm accurate reference tracking and show that the controller operates as intended on actual hardware.

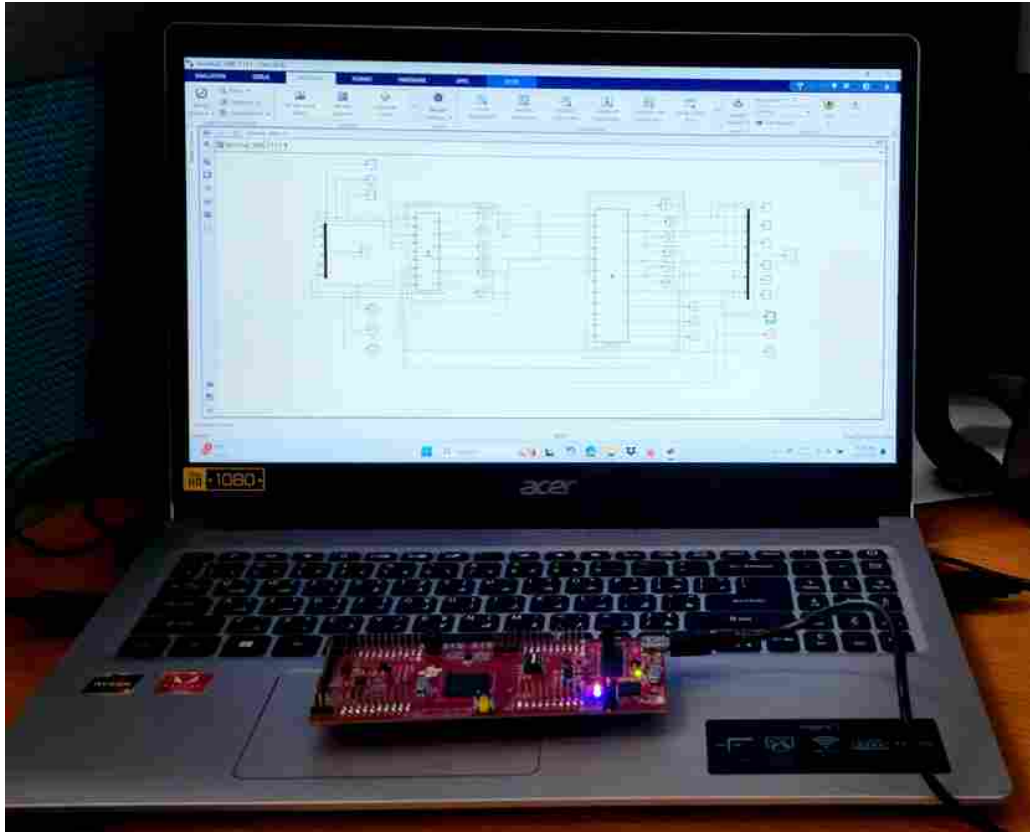


Figure 4.8: HIL Simulation System Display

4.2.1 Hardware-in-Loop Simulation Results

The trends observed in the HIL simulation graphs closely align with those from the continuous data simulations, confirming the reliability and robustness of the proposed controllers. These simulations validate the controllers' ability to achieve desired changes in physiological conditions in real-time.

The following graphs present a performance comparison of the six states (tumor cells, natural killer cells, CD8+ T cells, circulating lymphocytes, chemotherapy, and immunotherapy) across three dosage scenarios. Each graph illustrates that the controllers consistently maintain stability and effectiveness, ensuring convergence to the desired reference values within the expected timeframes. This consistency highlights the practical feasibility of implementing the controllers in hardware systems.

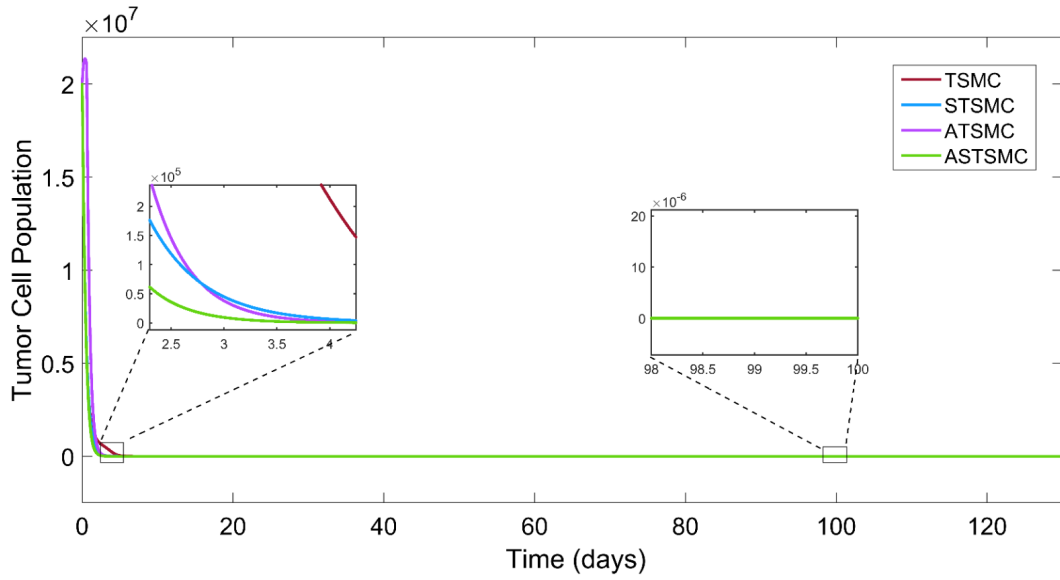


Figure 4.9: Tumor Cell Population Comparison Over Time.

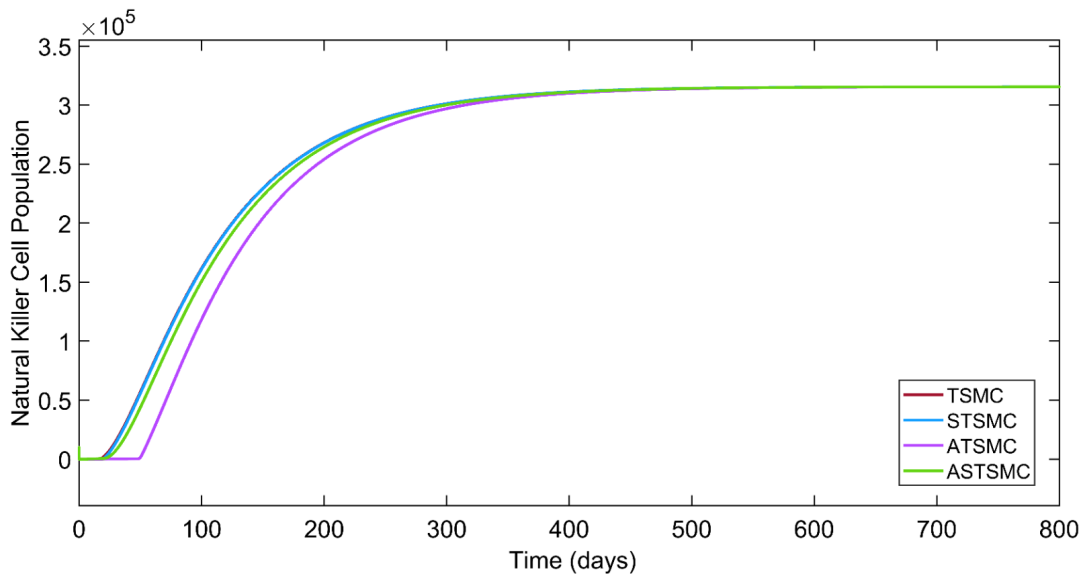


Figure 4.10: Natural Killer Cell Population Comparison Over Time.

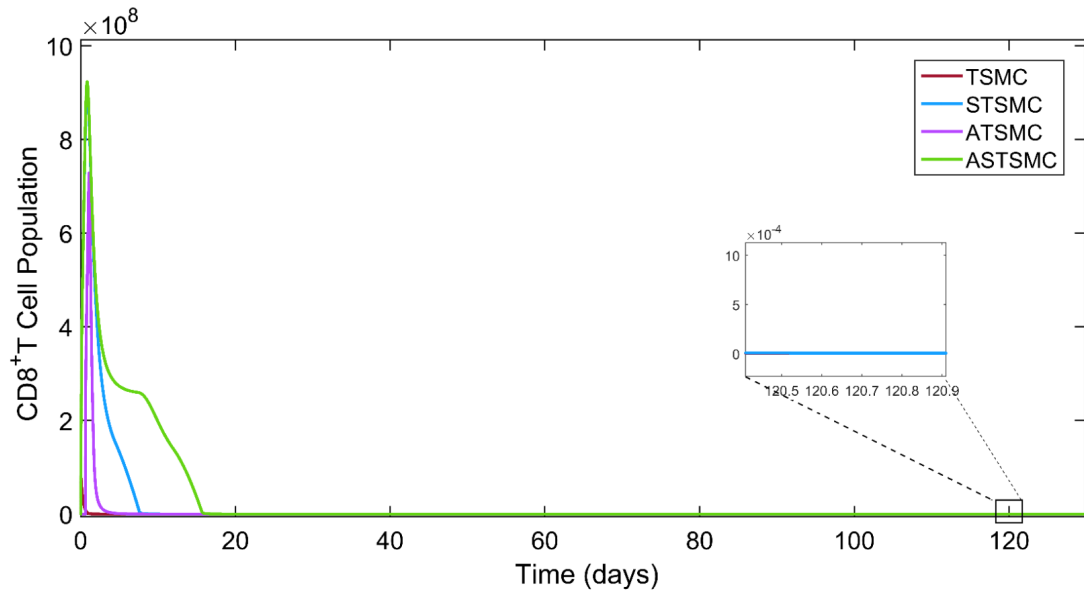


Figure 4.11: CD8⁺ T Cell Population Comparison Over Time.

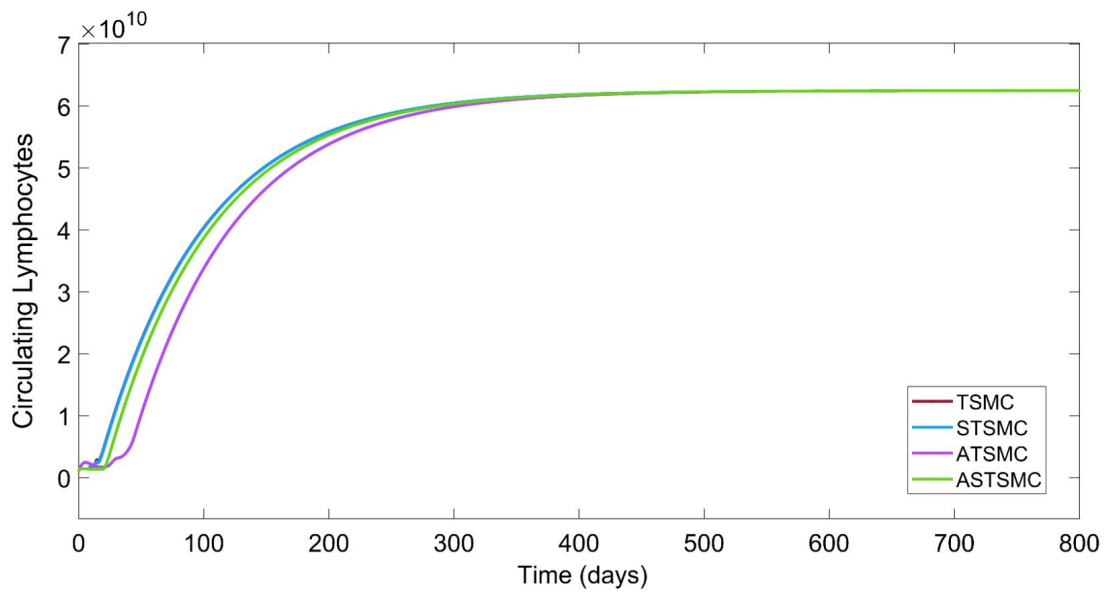


Figure 4.12: Circulating Lymphocytes Population Comparison Over Time.

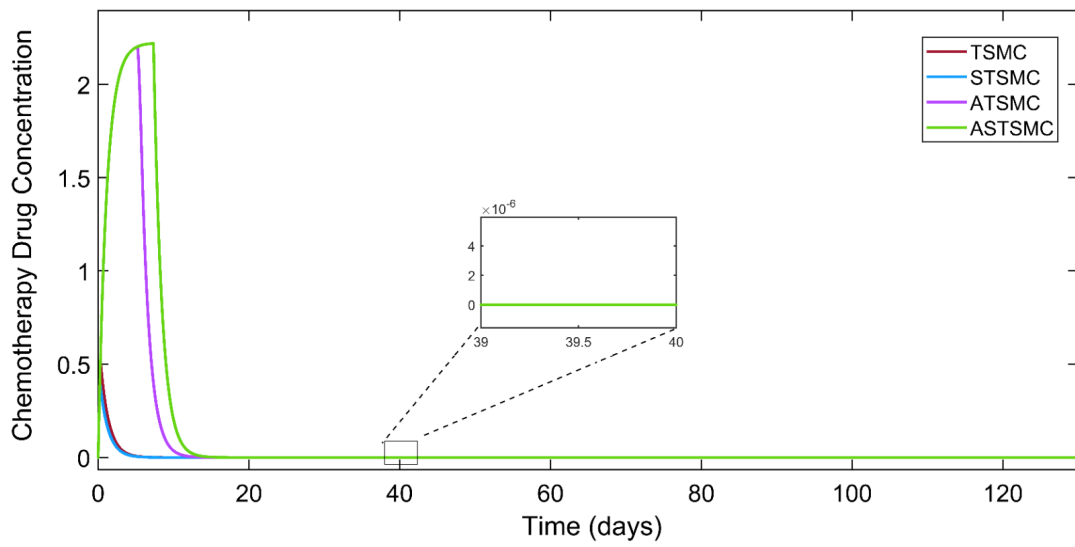


Figure 4.13: Chemotherapy Concentration Comparison Over Time.

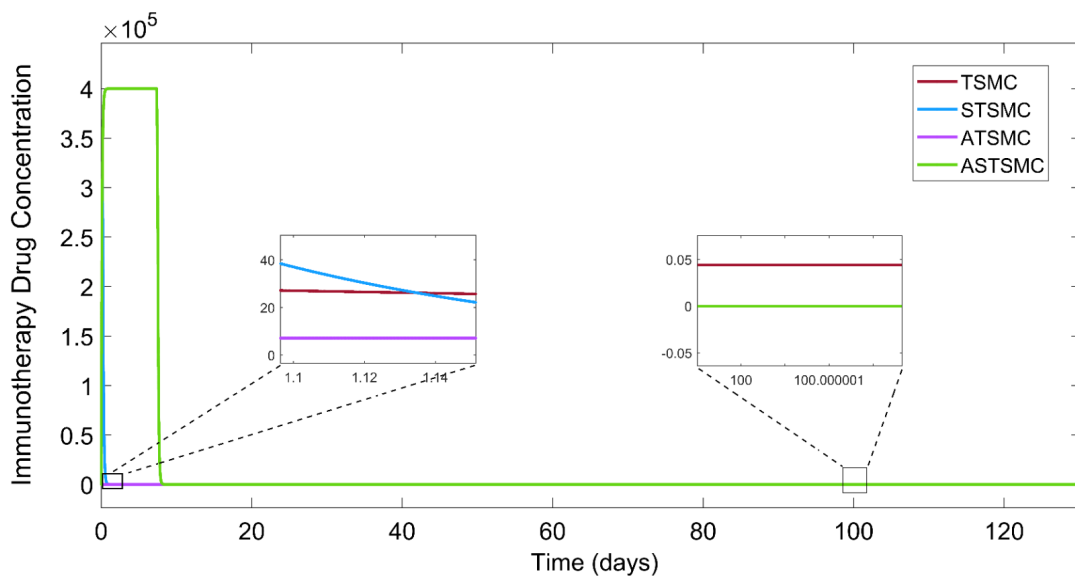


Figure 4.14: Immunotherapy Concentration Comparison Over Time.

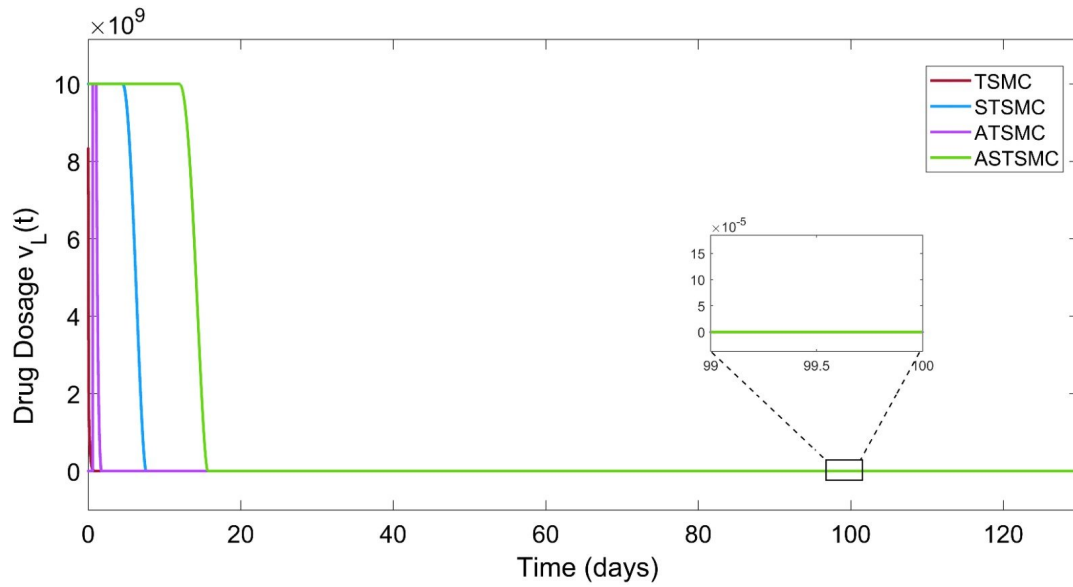


Figure 4.15: Immunotherapy Dosage (TIL): $v_L(t)$ Comparison Over Time.

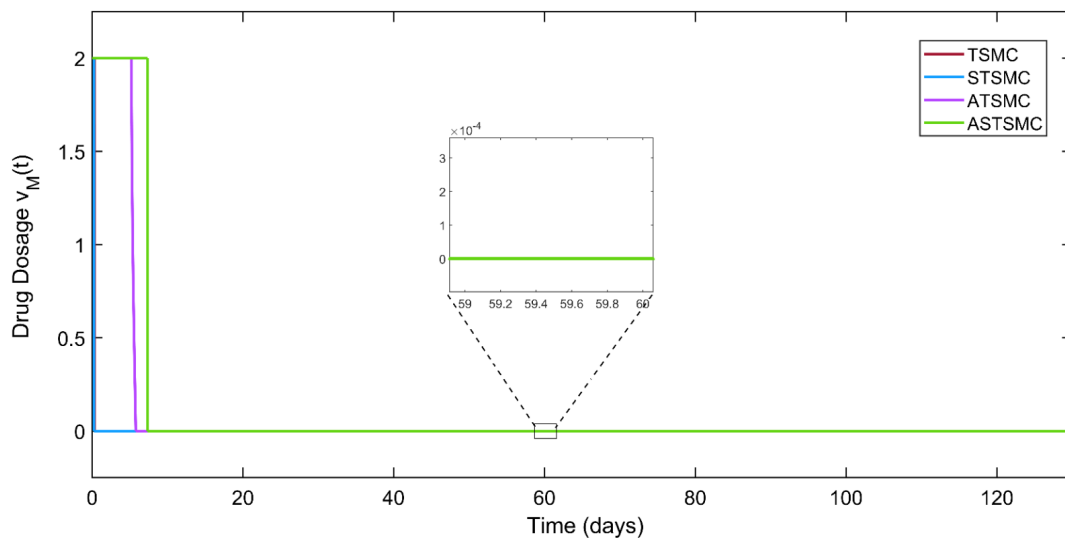


Figure 4.16: Chemotherapy Dosage: $v_M(t)$ Comparison Over Time.

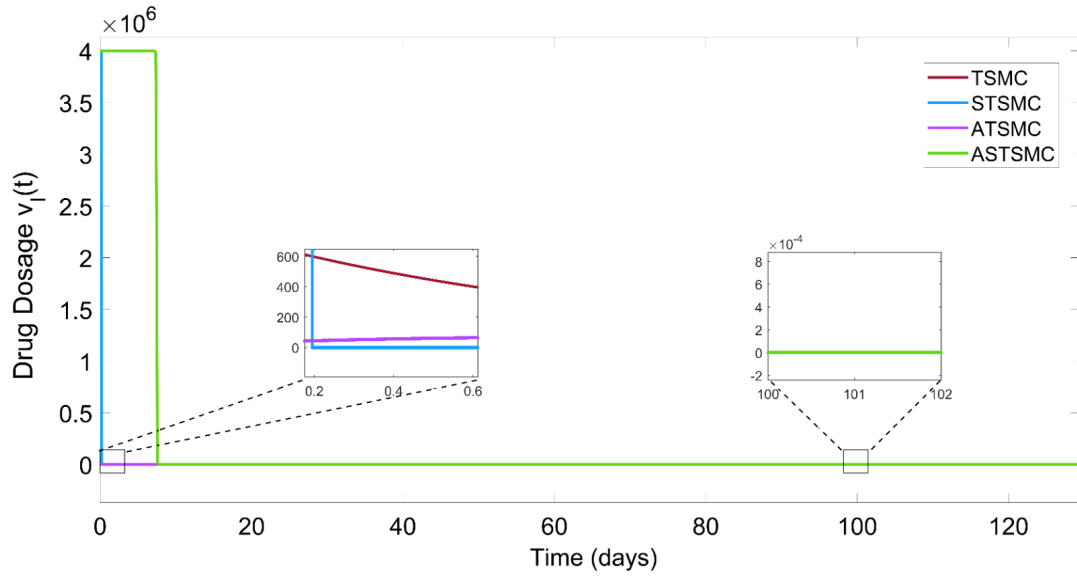


Figure 4.17: Immunotherapy Dosage (IL-2): $v_I(t)$ Comparison Over Time.

4.2.2 Benefits of Hardware-in-the-Loop (HIL)

Hardware-in-the-loop (HIL) testing is a vital approach used in many fields, including controller design, offering the following key benefits:

- **Realistic Simulations:** Combines real hardware with virtual scenarios for accurate testing.
- **Early Issue Identification:** Detects problems early for timely fixes before deployment.
- **Time and Cost Efficiency:** Cuts the need for prototypes and field testing, saving resources.
- **Smooth Component Integration:** Ensures seamless collaboration between hardware and software.
- **Versatility and Reusability:** Tests risky situations without endangering lives or equipment.
- **Improved Safety:** Allows testing in multiple scenarios and can be reused for future projects.
- **Performance Enhancement:** Optimizes system functionality through iterative testing.

Chapter 5

Conclusion And Future Directions

5.1 Conclusion

In this thesis, advanced nonlinear controllers such as Terminal Sliding Mode Control (TSMC), Super Twisting Sliding Mode Control (STSMC), Adaptive Terminal Sliding Mode Control (ATSMC), and Adaptive Super Twisting Sliding Mode Control (ASTSMC) were designed and applied to optimize drug delivery in mixed chemo-immunotherapy. The controllers were designed to minimize drug dosages, reduce treatment durations, and ensure rapid tumor regression while maintaining immune system health.

Among the proposed controllers, the Adaptive Super Twisting Sliding Mode Controller (ASTSMC) demonstrated the best performance, achieving tumor convergence to near-zero levels within 9 days. The parameters of all controllers were fine-tuned using the Improved Grey Wolf Optimization (IGWO) algorithm, with the Mean Squared Error (MSE) as the cost function. Stability was rigorously analyzed through Lyapunov theory to ensure reliable performance. The effectiveness of the controllers was validated through simulations conducted in MATLAB/Simulink and further verified in Hardware-in-the-Loop (HIL) experiments using the C2000 Delfino™ MCU F28379D Launchpad. The results demonstrated the ability of these controllers to stabilize tumor dynamics, reduce tumor cell populations, and maintain immune cell populations within desired limits.

The proposed approach outperformed existing methods, achieving faster tumor reduction, better immune recovery, and improved drug efficiency. The consistency between continuous and HIL simulations highlights the feasibility of implementing these controllers in real-world applications.

5.2 Scopes and Limitations

This study explores the application of advanced nonlinear controllers, including TSMC, STSMC, ATSMC, and ASTSMC, for optimizing drug delivery in mixed chemo-immunotherapy. The scope includes validating the controllers using MATLAB/Simulink simulations, analyzing drug and immune system dynamics through a six-state cancer model, and comparing the controllers to identify the most efficient approach for tumor suppression and immune recovery. Real-time feasibility was verified through Hardware-in-the-Loop (HIL) experiments using the C2000 Delfino™ MCU F28379D Launchpad.

However, the study has some limitations. The six-state model simplifies certain physiological complexities, excluding factors like tumor heterogeneity and microenvironment interactions. The results are parameter-dependent and not validated with patient-specific

clinical data. Additionally, the HIL implementation has hardware constraints, and long-term side effects, immune response variability, and therapy resistance remain unaddressed.

5.3 Further Research Work

Future work can focus on exploring additional advanced nonlinear control strategies, such as barrier-based nonlinear controllers and synergetic controllers. Additionally, optimization techniques like Red Fox Optimization (RFO) and improved Grey Wolf Optimization (I-GWO) with the Integral of Time-weighted Absolute Error (ITAE) as the cost function could be employed for parameter tuning to improve computational efficiency and accuracy. Furthermore, clinical validation through personalized patient data and extending the framework to real-time adaptive control systems could pave the way for practical and personalized cancer treatment strategies.

Bibliography

- [1] J Aroesty et al. “Tumor growth and chemotherapy: Mathematical methods, computer simulations, and experimental foundations”. In: *Mathematical Biosciences* 17.3-4 (1973), pp. 243–300.
- [2] Kashif Asghar, Asim Farooq, and Asif Loya. “Experiences of Shaukat Khanum Memorial Cancer Hospital and Research Centre Biobank during COVID-19 Pandemic”. In: *Asian Pacific Journal of Cancer Prevention: APJCP* 23.9 (2022), p. 2879.
- [3] Charles F Babbs. “Predicting success or failure of immunotherapy for cancer: insights from a clinically applicable mathematical model.” In: *American journal of cancer research* 2.2 (2012), pp. 204–213.
- [4] Marko Bacic. “On hardware-in-the-loop simulation”. In: *Proceedings of the 44th IEEE Conference on Decision and Control*. IEEE. 2005, pp. 3194–3198.
- [5] Maaly Bassiony, Adedoyin Victoria Aluko, and James A Radosevich. “Immunotherapy and cancer”. In: *Precision Medicine in Oncology* (2020), pp. 133–156.
- [6] “Cancer: Key Facts”. In: (2022). URL: https://www.who.int/health-topics/cancer#tab=tab_1.
- [7] Filippo Castiglione and Benedetto Piccoli. “Cancer immunotherapy, mathematical modeling and optimal control”. In: *Journal of theoretical Biology* 247.4 (2007), pp. 723–732.
- [8] Sophie Chareyron and Mazen Alamir. “Mixed immunotherapy and chemotherapy of tumors: feedback design and model updating schemes”. In: *Journal of theoretical biology* 258.3 (2009), pp. 444–454.
- [9] Julia Judd and Hossein Borghaei. “Combining immunotherapy and chemotherapy for non–small cell lung cancer”. In: *Thoracic surgery clinics* 30.2 (2020), pp. 199–206.
- [10] Jihoon Kim, Margaret P Manspeaker, and Susan N Thomas. “Augmenting the synergies of chemotherapy and immunotherapy through drug delivery”. In: *Acta biomaterialia* 88 (2019), pp. 1–14.
- [11] Denise Kirschner and John Carl Panetta. “Modeling immunotherapy of the tumor-immune interaction”. In: *Journal of mathematical biology* 37 (1998), pp. 235–252.
- [12] Vladimir A Kuznetsov et al. “Nonlinear dynamics of immunogenic tumors: parameter estimation and global bifurcation analysis”. In: *Bulletin of mathematical biology* 56.2 (1994), pp. 295–321.
- [13] Rein Luus, Frank Hartig, and Friedrich J Keil. “Optimal drug scheduling of cancer chemotherapy”. In: *Periodica Polytechnica Chemical Engineering* 38.1-2 (1994), pp. 105–109.

- [14] Seyedali Mirjalili, Seyed Mohammad Mirjalili, and Andrew Lewis. “Grey wolf optimizer”. In: *Advances in engineering software* 69 (2014), pp. 46–61.
- [15] Weiwei Mu et al. “A review on nano-based drug delivery system for cancer chemioimmunotherapy”. In: *Nano-Micro Letters* 12 (2020), pp. 1–24.
- [16] Global Cancer Observatory. *Cancer Today*. 2022. URL: https://gco.iarc.who.int/today/en/dataviz/pie?mode=cancer&group_populations=1&types=0.
- [17] Global Cancer Observatory. *Cancer Today - Detailed Statistics*. Accessed: YYYY-MM-DD. 2022. URL: https://gco.iarc.who.int/today/en/dataviz/pie?mode=cancer&group_populations=1&types=1.
- [18] Liuyong Pang, Lin Shen, and Zhong Zhao. “Mathematical modelling and analysis of the tumor treatment regimens with pulsed immunotherapy and chemotherapy”. In: *Computational and Mathematical Methods in Medicine* 2016.1 (2016), p. 6260474.
- [19] Lisette G de Pillis, Weiqing Gu, and Ami E Radunskaya. “Mixed immunotherapy and chemotherapy of tumors: modeling, applications and biological interpretations”. In: *Journal of theoretical biology* 238.4 (2006), pp. 841–862.
- [20] Lisette G de Pillis and Ami Radunskaya. “A mathematical model of immune response to tumor invasion”. In: *Computational fluid and solid mechanics 2003*. Elsevier, 2003, pp. 1661–1668.
- [21] Lisette G de Pillis, Ami E Radunskaya, and Charles L Wiseman. “A validated mathematical model of cell-mediated immune response to tumor growth”. In: *Cancer research* 65.17 (2005), pp. 7950–7958.
- [22] Hafsah Qaiser, Iftikhar Ahmad, and Muhammad Kashif. “Fuzzy, synergetic and non-linear state feedback control of chemotherapy drug for a cancerous tumor”. In: *Biomedical Signal Processing and Control* 62 (2020), p. 102061.
- [23] Adam I Riker et al. “Immunotherapy of melanoma: a critical review of current concepts and future strategies”. In: *Expert Opinion on Biological Therapy* 7.3 (2007), pp. 345–358.
- [24] Chandrashekhar M Sakode et al. “Multimodal therapy for complete regression of malignant melanoma using constrained nonlinear optimal dynamic inversion”. In: *Biomedical Signal Processing and Control* 13 (2014), pp. 198–211.
- [25] Mrinmoy Sardar, Santosh Biswas, and Subhas Khajanchi. “Modeling the dynamics of mixed immunotherapy and chemotherapy for the treatment of immunogenic tumor”. In: *The European Physical Journal Plus* 139.3 (2024), pp. 1–26.
- [26] N Sharifi, Sadjad Ozgoli, and Amin Ramezani. “Multiple model predictive control for optimal drug administration of mixed immunotherapy and chemotherapy of tumours”. In: *Computer methods and programs in biomedicine* 144 (2017), pp. 13–19.
- [27] Junjie Wu and David J Waxman. “Immunogenic chemotherapy: dose and schedule dependence and combination with immunotherapy”. In: *Cancer letters* 419 (2018), pp. 210–221.
- [28] Tianqian Zhang and Dorothee Herlyn. “Combination of active specific immunotherapy or adoptive antibody or lymphocyte immunotherapy with chemotherapy in the treatment of cancer”. In: *Cancer Immunology, Immunotherapy* 58 (2009), pp. 475–492.

- [29] Samira Zouhri et al. “Mixed immunotherapy and chemotherapy of tumors: optimal control approach”. In: *International Journal of Computer Science Issues (IJCSI)* 10.4 (2013), p. 81.
- [30] Muhammad Zubair, Iftikhar Ahmad, and Yasir Islam. “Backstepping and Synergetic Controllers for the Chemotherapy of Brain Tumor”. In: *International Journal of Control, Automation and Systems* 19.7 (2021), pp. 2544–2556.
- [31] Muhammad Zubair et al. “Lyapunov based nonlinear controllers for the chemotherapy of brain tumor”. In: *Biomedical Signal Processing and Control* 68 (2021), p. 102804.
- [32] Muhammad Zubair et al. “Variable structure based control for the chemotherapy of brain tumor”. In: *IEEE Access* 9 (2021), pp. 107333–107346.